AD _____

Award Number: W81XWH-08-1-0469

TITLE: (Enter title of award) MR Guided Pulsed High Intensity Focused Ultrasound Enhancement of Gene Therapy Combined with Androgen Deprivation and Radiotherapy for Prostate Cancer Treatment

PRINCIPAL INVESTIGATOR: Lili Chen, Ph.D.

CONTRACTING ORGANIZATION:
Institute for Cancer at Fox Chase Cancer Center
Philadelphia, PA 19111

REPORT DATE: September 2012

TYPE OF REPORT: Final

PREPARED FOR: U.S. Army Medical Research and Materiel Command
Fort Detrick, Maryland 21702-5012

DISTRIBUTION STATEMENT: (Check one)

✓ Approved for public release; distribution unlimited

Distribution limited to U.S. Government agencies only;
report contains proprietary information

REPORT DOCUMENTATION PAGE

Form Approved
OMB No. 0704-0188

1. REPORT DATE *(DD-MM-YYYY)*	2. REPORT TYPE	3 DATES COVERED *(From - To)*
September 2012	Final	01 September 2008 - 31 August 2012

4. TITLE AND SUBTITLE

MR Guided Pulsed High Intensity Focused Ultrasound Enhancement of Gene Therapy Combined with Androgen Deprivation and Radiotherapy for Prostate Cancer Treatment

5a. CONTRACT NUMBER

5b. GRANT NUMBER
W81XWH-08-1-0469

5c. PROGRAM ELEMENT NUMBER

6. AUTHOR(S)

Lili Chen, Ph.D.

5d. PROJECT NUMBER

5e. TASK NUMBER

5f. WORK UNIT NUMBER

7. PERFORMING ORGANIZATION NAME(S) AND ADDRESS(ES)

Fox Chase Cancer Center
Philadelphia, Pennsylvania 19111

8. PERFORMING ORGANIZATION REPORT

9. SPONSORING / MONITORING AGENCY NAME(S) AND ADDRESS(ES)

U.S. Army Medical Research and Materiel Command
Fort Detrick, Maryland 21702-5012

10. SPONSOR/MONITOR'S ACRONYM(S)

11. SPONSOR/MONITOR'S REPORT NUMBER(S)

12. DISTRIBUTION / AVAILABILITY STATEMENT

✓ Approved for public release; distribution unlimited
Distribution limited to U.S. Government agencies only - report contains proprietary information

13. SUPPLEMENTARY NOTES

14. ABSTRACT

This work aimed to test the hypothesis that MR guided pulsed HIFU exposures enhance gene delivery and increase the efficacy of gene therapy in inhibiting prostate cancer growth *in vivo*, particularly when combined with AD or RT. We developed techniques for the treatment of prostate tumor-bearing mice using a clinical MRgHIFU device. We performed animal studies for quantitative measurement of the doxorubicin concentration in HIFU treated prostate tumors to evaluate the "optimal" ultrasonic parameters derived from experiments using an acoustic phantom. We also performed experiments on the efficacy of MRgHIFU enhancement of docetaxel delivery combined with RT in inhibiting prostate tumor growth in vivo. We investigated the MRgHIFU effect on the enhancement of gene therapy using AS-MDM2 and bcl-2 in implanted prostate tumors in mice *in vivo* by measuring the protein expression level of MDM2, p53 and p21 using immunohistochemical staining and west blotting techniques. We also performed experiments on the efficacy of MRgHIFU enhancement of AS-MDM2 delivery in inhibiting prostate tumor growth in vivo. Our results show that MRgHIFU is safe and effective for the enhancement of drug delivery in prostate tumor.

15. SUBJECT TERMS

MR-guided pulsed focused ultrasound, prostate cancer, in vivo, drug delivery based treatment planning

16. SECURITY CLASSIFICATION OF:			17. LIMITATION OF ABSTRACT	18. NUMBER OF PAGES	19a. NAME OF RESPONSIBLE PERSON
a. REPORT	b. ABSTRACT	c. THIS PAGE			USAMRMC
U	U	U	UU	39	19b. TELEPHONE NUMBER

Standard Form 298 (Rev. 8-98)
Prescribed by ANSI Std. Z39.18

Table of Contents

Introduction

Due to the unforeseeable reasons described in the first-year report our animal study was delayed by one year. A request for one year no-cost extension was approved by DOD.

The specific aims include (1) To determine if HIFU increases the cellular uptake of AS-MDM2, AS-bcl-2 and AS-PKA, thereby suppressing MDM2, bcl-2 and PKA, respectively, *in vivo* (2) To determine if HIFU enhances the uptake of adenoviral-E2F1 (Ad-E2F1), and (3) To establish whether the increased uptake of AS-MDM2 enhances tumor growth inhibition when combined with AD or RT. The detailed experimental procedures and results are summarized below.

Body

In this final report we summarize our accomplishments associated with the tasks outlined in the approved "Statement of Work" in the proposal. We have performed studies to determine if HIFU increases the cellular uptake of AS-MDM2, AS-bcl-2 thereby suppressing MDM2, bcl-2 respectively, *in vivo.* The sequence of our studies, leading up to the gene delivery experiments is as follows. First, we performed experiments on a phantom that was provided by InSightec to determine the ultrasonic treatment parameters including the frequency, acoustic power, duty cycle and exposure duration for drug delivery enhancement studies without damaging normal tissues. Second, we developed techniques for the treatment of prostate tumor-bearing mice using a clinical MRI-guided HIFU (MRgHIFU) treatment device. Third, we evaluated the ultrasonic parameters derived from the acoustic phantom experiment for drug enhancement delivery in prostate tumors in mice using doxorubicin. Fourth, based on the in vivo results that drug concentration of doxorubicin is increased in the HIFU treated prostate tumors we investigated the MRgHIFU effect on the enhancement of AS-MDM2, bcl-2 (gene therapy) in implanted prostate tumors in mice *in vivo* by measuring the protein expression level of MDM, p53 and p21 with time points after treatment using immunohistochemical staining and west blotting. We also performed experiments to establish the efficacy of AS-MDM2, in inhibiting prostate tumor growth in vivo. Our in vivo animal results did not show significant therapeutic effects on tumor growth control using AS-MDM2. This could be the result of either ineffective gene agents or suboptimal HIFU parameters that did not enhance the drug delivery. Further animal studies were carried out using a chemotherapeutic drug, docetaxel, which has been routinely used for treatment of prostate cancer patients clinically with proven therapeutic effects to increase patient survival. We performed quantitative measurements of 3H-docetaxel concentration in implanted tumors with and without HIFU treatment, which clearly demonstrated the drug delivery enhancement using our MRgHIFU parameters. We also demonstrated the efficacy of increased 3H-decetaxel with MRgHIFU using our established treatment parameters in inhibiting prostate tumor growth in vivo and combined with RT. Based on these extensive animal studies we have published 3 peer reviewed papers in Phys. Med. Biol and Med. Phys (1-3), both are top radiation physics and biology journals, and numerous abstracts presented in the national and international conferences. Two peer reviewed abstracts were selected as the best papers presented at the AAPM annual meeting 2012 and published in the journal of Med. Phys (4-5). We summarize the results from these studies in the following sections.

To determine if HIFU increases the cellular uptake of AS-MDM2, AS-bcl-2 and AS-PKA, thereby suppressing MDM2, bcl-2 and PKA, respectively, *in vivo*.

Characterization of the output of the focused ultrasound unit using MR guidance

Study of ultrasound output parameters on phantom

A series of pilot experiments were performed on an MRgHIFU system (An ExAblate 2000 HIFU system, InSightec, Inc. and a 1.5 T MR scanner, GE) with an acoustic phantom provided by InSightec. The purpose of these studies were to determine the ultrasound parameters including frequency, acoustic power and pulse width that are adequate for the enhancement of gene therapy for the treatment of prostate cancer in mice, without causing damage to overlapping healthy tissues permanently. The MR proton resonance frequency shift sequence was used for temperature monitoring during the treatment. We assumed that tissue would not be damaged below 42°C. In order to avoid permanent tissue damage the temperature elevation should be below 5 °C based on the animal ambient temperature. Our results suggested that in order to avoid permanent tissue damage, the acoustic power should be below 5 W and the temperature elevation < 4°C. With these ultrasonic treatment parameters, we have further demonstrated that there were no ultrasonic lesions seen in ex-vivo tissue. The 1 MHz frequency was chosen based on the cavitation mechanism, which has been discussed in the literature (6-7).

We also performed studies on the relationship between acoustic energy (acoustic power x ultrasonic exposure time) and the temperature elevation for a given acoustic power of 4 W. Results showed that 4 °C temperature elevation is maintained from 40 joule (exposure time 10 s) to 240 joule (exposure time 60 s) due to the thermal equilibrium. It is expected that although the temperature elevation is the same for this acoustic energy range the biological effects in animals (*in vivo)* may be different. These phantom measurements provided basic ultrasonic parameters for the *in vivo* studies. The ultrasound treatment parameters including frequency: 1MHz, duty cycle: 50% and exposure duration: 60 seconds were used in our pilot in vivo animal studies (see below).

Determination of tumor model and the optimal MR protocols

All *in vivo* pilot studies were carried out in compliance with guidelines and approval of both the IACUC and DOD ACURO (08-19). The human prostate cancer cell line, LNCaP (wild-type) was used for the study (8). LNCaP cells (1×10^6) were injected into the prostates of mice orthotopically. Tumor growth was monitored weekly on MRI starting 3 weeks after the implantation. MR imaging was also used for ultrasonic treatment guidance including tumor target delineation, treatment planning, and real-time localization for ultrasonic beam delivery.

An optimal MR imaging protocol was developed, which allows us to obtain a higher quality image to visualize the prostate tumor in the small animal while the scan time remains acceptable for the whole MRgHIFU treatment procedure to be within the approximate 1h anesthesia time. A three-inch surface coil was used. A quick scan was performed for initial localization using the fast spin echo (FSE) image sequence at low image quality. The scan time was 0.13 min. It was followed by a high quality image sequence with 7 min scan time in order to identify the tumor target. The MR parameters were: T2-weighted coronal fast spin echo (FSE) sequence; TR/TE=2150/102 ms; Bandwidth: 10.4 kHz; FOV=9 x 9 cm; Matrix: 384 x 384 NEX: 4; slice thickness: 2.0 mm/0.0 sp; frequency direction: SI and the spatial resolution: 0.23 mm. Based on the coronal image, an axial MR sequence was performed with 4.25 min. The total scan time was approximately 12 minutes, which allows us to complete the entire HIFU treatment procedures in an hour. These animal experimental procedures will be useful to future in vivo studies on MRgHIFU drug enhancement for cancer therapy.

Development of experimental techniques for animal studies in vivo using FDA approved clinical MRgHIFU system

Prior to treatment a quality control (QC) procedure was performed to check the automatic electronic motion system, the transducer output, and the effective focal region using acoustic phantom. The mice were treated under general anesthesia using a mixed solution of Ketamine at 60 mg/kg & Ace-promazine at 2.5 mg/kg in 15 micro liters total volume by intraperitoneal (i.p.). A gel phantom was

placed on the treatment table in line with the transducer. Degassed water was used for the interface between the treatment table and the gel phantom for the acoustic coupling. Care was taken to eliminate any air bubbles between the interfaces. The gel phantom was warmed to approximately 37 °C and a shallow hole measured about 2cm x 3cm with 8 mm in depth was made. The hole was located in the center on the top of the gel and filled with warm degassed water. The animal was carefully placed on the gel phantom in contract with the degassed water in a prone position. A 3-inch surface coil was placed around the animal to receive the MR signals. A small acoustic phantom was placed beside the mouse for the purpose of the beam focus verification. A small warm water bag was placed on the animal to keep its body temperature. Three localization MR sequences were performed. The interface between the phantom and animal skin was carefully checked on MR images for the gas bubbles. The animal was removed immediately after the HIFU treatment. The Mice were warmed, monitored and allowed to recover from anesthesia (1).

Evaluation of the ultrasonic parameters derived from the acoustic phantom for enhanced drug delivery in prostate tumors in mice using doxorubicin.

A pilot study was performed on mice with human prostate cancer grown orthotopically to test if MRgHIFU increases cellular uptake of doxorubicin (American Pharmaceutical partners, Inc., Los Angeles, CA) by measuring the fluorescence quantitatively. The average of tumor volume was 160 ± 27 mm^3, as measured by MR. Eight animals were used for this study. The first group included 3 mice. The first mouse was used for MRgHIFU+ doxorubicin (10 mg/kg); mouse 2 was used for doxorubicin (10 mg/kg) injection only and mouse 3 was used as a control. The second group included 4 mice. Mice 1 and 2 were used for MRgHIFU+ doxorubicin (10 mg/kg), and mice 3 and 4 were used for doxorubicin injection (10 mg/kg) only. We also used one animal for MRgHIFU + doxorubicin (20 mg/kg). Note that here we increased the doxorubicin dose from 10 mg/kg to 20 mg/kg to compare if the doxorubicin uptake increases with dose.

The animal was treated with pulsed ultrasound using 1 MHz; 4 W of acoustic power, pulse width 0.1 s, and duty cycle: 50% (5 Hz frequency with 0.1s power on, 0.1s power off) for 60 seconds. During the MRgHIFU treatment, phase MR images were used for measurement of the temperature in the focal spot. It was found that the temperature elevation was below 4 °C based on MR thermometry for the ultrasonic parameters used. The time for the whole treatment procedure took approximate 1 h. All animals tolerated well to ultrasound treatment. No skin toxicities were observed in any animals treated.

In our study, doxorubicin (10 mg/kg or 20 mg/kg) was injected by tail vein immediately after the MRgHIFU treatment. Animals were sacrificed 2 hr after the injection. The determination of the 2 hr time point was based on the assumption that 2 hours after the injection the drug would be effectively accumulated in the tumor via blood circulation. Tumors were harvested and split, such that one half was snap frozen and cut at 5 μm thick for fluorescent images and the other half was prepared to quantify fluorescent tracers. Fluorescence of the lysate was measured by a fluorometer (λ_{ex} = 485 nm, $\Delta\lambda_{em}$ = 538 nm). Our data showed that the concentration of doxorubicin in the treated tumors was increased in the MRgHIFU treated group (n=3) compared with those without MRgHIFU group (n=3). We did not find higher uptake for the mouse injected with a higher (20mg/kg) doxorubicin dose (data not shown). Our results also showed that the distribution of doxorubicin was increased in tumors treated with MRgHIFU.

Determination of the uptake of AS-MDM2 in orthotopically grown LNCaP tumors in vivo

Based on the pilot study described above with increased uptake of doxorubicin in HIFU treated animals we initiated an in vivo study to determine the cellular uptake of AS-MDM2 with MRgHIFU in vivo. Human prostate cancer cells LNCaP ($1x10^6$) were grown orthotopically in the prostates of 28 nude mice. Twenty-eight mice were divided randomly into 4 Groups (n=7/group): Group 1:

MRgHIFU+AS-MDM2; Group 2: AS-MDM2 alone; Group 3: MRgHIFU alone; Group 4: control. The mice bearing implanted prostate tumors were treated under general anesthesia. The tumors were treated with the acoustic power of 4 W, pulse width of 0.1 seconds, 50% duty cycle and 60 s (300 pulses) in one sonication. The focal peak was set within the target under the MR guidance. Multiple sonications were used depending on the tumor size to cover the whole tumor. Immediately after the ultrasound treatment 0.1 ml of AS-MDM2 (Microbac Laboratories, Inc), dissolved in PBS, was given by tail vein injection at doses 25 mg/kg for Groups 1 and 2.

Mice were sacrificed 6 and 24 hr after injection of AS-MDM2 regardless of whether or not they were exposed to MRgHIFU. The tumors were removed and fixed in 10% buffered neutral formalin and paraffin-embedded for assessment of protein expression by mmunohistochemical staining. The expression levels of MDM2, p53 and p21 proteins were quantified using an image-analysis system (ACIS, Chromavision Medical Systems, Inc., San Juan Capistrano, CA). Our results showed that there were no significant differences between groups treated with and without MRgHIFU both 6 hours and 24 hours after the MRgHIFU treatment although we observed blood cell extravasations on H&E staining in the MRgHIFU treated tumors, as compared to other groups. It seemed that one single AS-MDM injection did not knock down MDM2 or result in an increase in p53 and p21. Since it was not certain as whether the immunohistochemical staining results accurately reflect the effects of AS-MDM2 (either due to measurement threshold or timing), we proceeded with direct outcome measurements. The effect of multiple MRgHIFU and AS-MDM2 treatments on the inhibition of LNCaP tumor growth was measured subsequently (see below).

To establish the efficacy of increased AS-MDM2 in inhibiting prostate tumor cell growth in vivo

There were 3 groups with 7 LNCaP-bearing mice per group. The 3 groups were: Group 1, MRgHIFU + AS-MDM2, Group 2, AS-MDM2 alone, and Group 3, Sham MRgHIFU. The experimental procedures were as follows:

Group 1: When tumor grew to the size about 60 mm^3 (about 4 mm in diameter), as determined by MRI, we started to treat with MRgHIFU for 6 treatments over three weeks (2 treatments per week, i.e., Monday and Friday). Each treatment was followed by an i.p. injection of AS-MDM (25 mg/kg) immediately after each MRgHIFU treatment. The dose of AS-MDM2 was determined based on our previous study (3).

Group 2: AS-MDM2 alone (25 mg/kg) was administered for 6 treatments over three weeks (2 treatments per week, i.e., Monday and Friday).

Group3: These tumor-bearing mice comprised the sham MRgHIFU group.

The tumor growth for each group was determined by measuring the tumor volume by MRI. The tumor volume was collected weekly for each mouse after initiating the treatment. The mice were sacrificed when tumor reached about 600 mm^3 or 7 weeks after treatment whichever comes first. Our results showed that there were no significant differences between the groups with and without MRgHIFU treatment.

Determination of the uptake of AS-bcl-2 in orthotopically grown LNCaP tumors

In parallel, we also performed experiments to determine the optimal uptake of AS-bcl-2 in orthotopically grown LNCaP tumors. The prostate tumor was exposed to HIFU using optimal ultrasound parameters derived from our phantom study. The antisense agents (25mg/kg) were injected by tail vein immediately after the HIFU exposure. There were 3 groups: Group 1, control; Group 2, AS-bcl-2 injection (by tail vein) alone, tumors were removed at 4 hr, 6 hr, 12 hr, 24 hr, 48 hr and 72 hr after a single treatment respectively; and Group3, HIFU + AS+bcl-2 with tumor removed at 24 h after a single treatment. The tumors in Group 3 were treated using HIFU with the the following parameters:

acoustic power of 4W, pulse width of 0.1 sec, 50% duty cycle and 1 minute exposure duration (300 pulses per sonication) for one sonicaion. Multiple sonications were used (up to 10 sonications) to cover the whole tumor volume depending the tumor size. Mice were sacrificed at predetermined time points. Tumors were removed and one part snap frozen for Western blot analysis using anti-bcl-2 mouse monoclonal antibody (clone 124, DAKO, Carpinteria, CA) at 1:500 dilution and anti-beta actin antibody (Calbiochem, San Diego, CA) as a loading control at 1:5000 dilution, and the other part fixed in formalin and paraffin-embedded for immunohistochemical (IHC) analysis using anti-bcl-2 (1:50 dilution) and anti-p53 mouse monoclonal antibody (clone DO-7; DAKO) (1:200 dilution). Frozen tumors were homogenized and lysed on ice. Protein samples from each experimental group were mixed and pooled together. Protein concentration was determined using the BCA protein assay. 30μg of total protein was fractionated by SDS-PAGE electrophoresis and transferred to PVDF membranes. Primary antibody incubation was carried out overnight at 4˚C; membranes were then washed and incubated with secondary antibody for 1 hour at room temperature. Proteins of interest were detected using the ECL detection kit (Pierce).

As shown by Western blot analysis (see our second report) there was no change in Bcl-2 protein expression among different groups and time points. Antisense treatment did not cause a reduction in Bcl-2 protein levels. The protein levels were uniform between the groups. We therefore examined the protein expression in these tumors by immunohistochemistry (IHC).

Measurement of Bcl-2 and p53

Protein expression levels were quantified using an image-analysis system *Aperio ScanScope* (Aperio Technologies Inc., Vista, CA). The IHC slides were converted to digital images with the ScanScope CS slide scanner and the automated quantification of staining was performed using the ImageScope Analysis Software, version 9 (Aperio), analogous to clinical pathology methods. On average 10 random areas in the tumor tissue containing tumor cells were analyzed under a 20x magnification.

Our results showed that Bcl-2 expression was low in all groups (ranged from 0.4% to 0.9% on average) and no significant differences between the treatment groups and time points. This is in agreement with the western blot data. No down-regulation of Bcl-2 was observed in prostate tumors with AS-Bcl-2 or AS-Bcl-2+HIFU treatments, which may be due to a low level of expression of Bcl-2 in these tumors.

Since our study results from both AS-MDM2 and AS-Bcl2 showed statistically insignificant differences in AS-MDM2 and Bcl2 uptake between groups treated with and without MRgHIFU at different time points there were no significant differences in tumor growth delay between the groups with and without MRgHIFU treatment with AS-MDM2 experiments, a series of experiments were further conducted to answer the question as whether the negative results were caused by the ineffectiveness of AS-MDM and AS-Bcl2 or by sub-optimal focused ultrasound treatment parameters used in our experiments. Experiments were performed using chemo therapeutic agents, Docetaxel and Doxorubicin (Dox) as those agents have been clinically proven to be effective in prostate cancer therapy. We summarized these studies below.

Study of intratumoral uptake of [3H]-docetaxel in vivousing MRgHIFU

In order to answer the question as whether the negative results were caused by the ineffectiveness of AS-MDM or inadequate focused ultrasound treatment parameters used in our experiments we performed extensive animal studies using docetaxel.

Docetaxel, either as a single agent or combined with others, has shown a survival benefit in prostate cancer patients. It has been routinely used in the clinic for the treatment of advanced hormone refractory prostate cancer (9-10) and other tumors (11-12). Docetaxel is also a potent radio-sensitizer (13). The purpose of this study was to investigate the possibility of the enhancement of [3H]-docetaxel uptake in prostate tumors implanted orthotopically using pulsed (MRgHIFU) using the same HIFU treatment parameters used for gene therapy described above. The rationale of the study is that if the delivery of 3H-docetaxel is enhanced in the treated prostate tumor then the insignificant results from the gene therapy experiments would be due to the ineffectiveness of the gene drug rather than HIFU treatment parameters that we used.

Animal treatment

When the tumor volume reached 140±10 mm^3 on MRI, MRgFUS treatment was performed. The tumor-bearing animals were randomly divided into three groups (n = 8 per group). The three groups are group 1, MRgFUS treatment + [^{3}H]-docetaxel i.v. injection (by tail vein); group 2, [^{3}H]-docetaxel i.v. injection only; and group 3, as control. For group 1, each mouse was treated with MRgFUS. MR images were used for target delineation, treatment planning and monitoring of temperature elevation during treatment. Immediately after ultrasound treatment, the animal received a single dose of i.v. injected docetaxel (Taxotere; sanofi-aventis U.S. LLC, Bridgewater, NJ) at 15mg/ kg mixed with [3H]-docetaxel (American Radiolabeled Chemicals, Inc.) at 50 μCi/kg in a total volume of 150 μl (9). Animals in group 2 were treated the same as in group 1, however without the MRgFUS treatment. Animals in group 3 were served as control. Animals were euthanized 30 min after i.v. injection with or without the MRgFUS treatment, and tumors were removed and processed.

Animals were treated with pulsed ultrasound using 1 MHz, 4W acoustic power and the 81 mode setting (5 Hz frequency with 0.1s power on, 0.1 s power off) for 60 s for each sonication (the same as for AS-MDM2 and AS-Bcl2). The time-averaged acoustic focal intensity was approximately 220W cm^2 determined based on the acoustic power and the beam cross-sectional area. The whole tumor volumes were covered with multiple focal spots (6–8 spots) depending on the tumor size.

Drug assay in tumor

The animal was euthanized 30 min after i.v. injection. The determination of the timing was based on the assumption that 30 min after drug administration, there would be reasonable drug concentration in the tumor volume through blood circulation. The tumor was removed, weighted and placed in a vial. The solvable solution (PerkinEkmer, Boston, MA) was added in the vial with a concentration of 12 μl/ mg for tumor sample digestion. The vial was suspended in a water bath at a temperature of 55 °C for 1 h. The vial was placed on the fisher vortex for convolution. Immediately after the convolution, the tumor solute sample of 900 μl (contain 75 mg tumor weight) was drawn and placed into a new vial. The new vial was given 0.2 ml of 30% hydrogen peroxide for 30 min at 55 °C for discoloration. ScintiverseTM BD cocktail of 10 ml was added in the vial for 1 h. The radioactivity of [3H]-docetaxel in the tumor tissue was then quantitatively measured by a liquid scintillation counter.

Statistical analysis

Statistical analysis was performed using SPSS (Statistical Package for the Social Sciences). Statistical significance among experimental groups was determined using the one-wayANOVA least significance difference (LSD) test. A p-value of <0.05 was considered to be significant.

The study results demonstrated increased [3H]-docetaxel concentration in tumors in the MRgFUS-treated group (1079 ± 132 cmp/75 mg) versus those without the MRgFUS treatment (524 ±201 cmp/75 mg) with $P = 0.037$. The results were analyzed over 34 mice, which showed initial tumor volumes in the range from 123 to 246 mm^3. Mice with lager tumor volumes (greater than 140 ±10 mm^3) were excluded to minimize the dose heterogeneity in the tumor volume due to hypoxia and center tumor necrosis. In the model system proposed, MRgFUS is hypothesized to improve the delivery of docetaxel into human prostate tumors grown orthotopically in nude mice. Our results indicated that it is true that docetaxel delivery in implanted tumors can be enhanced by focused ultrasound and MRI played an important role in on-line target delineation, treatment planning and treatment effect monitoring. The significance of our study is not only to demonstrate the enhancement of the docetaxel delivery in prostate tumor using focused ultrasound but more importantly to demonstrate a technique that is capable of performing studies on a small animal model using a clinical treatment system. These results will be helpful to other investigators who have the same treatment systems to perform clinical translational studies on the fast track. This study was published in the journal of Phys. Med. Biol (3). Based on our publication and presentations in conferences we have helped other institutions such as UCLA, City of Hope, etc. in applying our experimental techniques for small animal studies on drug delivery.

Based on the evidence of the 3H-docetaxel enhancement using MRgHIFU we also evaluated the efficacy of the enhancement of docetaxel by pulsed MRgHIFU in combination with radiotherapy (RT) for treatment of prostate cancer *in vivo*. LNCaP cells were grown in the prostates of male nude mice. When the tumors reached a designated volume by MRI, tumor bearing mice were randomly divided into seven groups ($n = 5$): (1) MRgHIFU alone; (2) RT alone; (3) docetaxel alone; (4) docetaxel + MRgHIFU; (5) docetaxel + RT; (6) docetaxel + MRgHIFU + RT, and (7) control. MR-guided HIFU treatment was performed using our MRgHIFU system. Animals were treated once with MRgHIFU, docetaxel, RT or their combinations. Docetaxel was given by i.v. injection at 5 mg/ kg before MRgHIFU. RT was given 2 Gy after MRgHIFU. Animals were euthanized 4 weeks after treatment. Tumor volumes were measured on MRI 1 and 4 weeks post-treatment. Results showed that triple combination therapies of docetaxel, MRgHIFU and RT provided the most significant tumor growth inhibition among all groups, which may have potential for the treatment of prostate cancer due to an improved therapeutic ratio. This study has been published in the journal of Phys. Med. Biol (2).

Based on our studies above, it is evident that MR guided pulsed HIFU can be used for enhancement of drug delivery in the prostate tumors without damaging to normal tissues. More studies are warranted on the mechanisms and the optimal treatment parameters to maximize the drug delivery enhancement. In order to study the optimal treatment conditions we have done further studies on both acoustic phantom and animals, as described below.

Quantitative study of focused ultrasound enhanced doxorubicin delivery to prostate tumor in vivo with MRI guidance

The purpose of this study was to study the optimal MRgHIFU treatment parameters to maximize the drug delivery enhancement. Doxorubicin was chosen for this study not only because it is an antitumor drug but also it is inherent with fluorescent property that can be used for accurate measurement of the drug concentration in excised tumor tissues quantitatively. In addition, it can be also used for the determination of spatial drug distributions using fluorescent images as demonstrated in our pilot study.

We expected to see similar effects as those obtained with 3H-docetaxel. Hypothesis: reliable treatment conditions will be reproducible and the drug enhancement effect can be quantified using independent measurement techniques.

First, experiments on a tissue mimic phantom to determine the optimal acoustic power and exposure durations with a 10% duty cycle and a 1 Hz pulse rate were performed. The temperature variation was monitored using real-time MR thermometry. With the given duty cycle of 10%, pulse rate 1 Hz, and acoustic frequency 1 MHz, the phantom was sonicated with various acoustic powers ranging from 10 to 50 W and sonication durations ranging from 10 to 60 s in 10 W and 10 s increments, respectively. The temperature elevations in the focal zone were measured for each pair of parameters (i.e., acoustic power and sonication duration) using MR thermometry, which is a machine built-in software function. The relation of the temperature elevation to acoustic power and exposure duration was plotted by bilinearly interpolating the measured data.

Second, tumor-bearing animals were treated with MRgHIFU. There were three groups (n=8/group): group 1 received MRgHIFU +Dox (10 mg/kg i.v. injection immediately after MRgHIFU exposure), group 2 received Dox only (10 mg/kg i.v. injection), and group 3 was a control. Tumor-bearing mice from group 1 were exposed to MRgHIFU using the following parameters: 1 MHz ultrasound, 25 W acoustic power, and 1 Hz pulse rate with a 10% duty cycle for 60 s for each sonication spot. A total of four to eight sonication spots were used to cover the entire tumor volume depending on the tumor size. The MRgHIFU parameters were selected based on our tissue phantom study. We believe that with the same temperature elevation (<5C) by using higher acoustic power with short exposure duty cycle will achieve better enhancement of drug livery. Tail vein injections (volume of 100μl) of Dox (10 mg/kg) were given to mice in group 1 immediately after MRgHIFU exposure (within 10 min). Group 2 received the same Dox injection, but without MRgHIFU exposure. No treatment was given to the control animals. Animals were euthanized 2 hrs after the MRgHIFU treatment. The Dox concentration in the treated tumors was measured by quantifying fluorescent tracers using a fluorometer (3).

Third, the histological changes of tumors with and without MRgHIFU treatments were evaluated. Finally, experiments were performed to study the spatial drug distribution in tumors after the MRgHIFU treatment, in which two animals received MRgHIFU +Dox, two animals received Dox only, and one animal was used as control. Two hours following the treatment, animals were euthanized and processed. The Dox distribution was determined using a fluorescence microscope.

Results: Our parametric measurements using a tissue phantom showed that the temperature increased with an increasing acoustic power (from 10 to 50 W) or sonication duration (from 10 to 60 s) with a given acoustic frequency of 1 MHz, duty cycle 10%, and pulse rate 1 Hz. A set of ultrasound parameters was identified with which the temperature elevation was less than 5 °C (11), which can be used for nonthermal MRgHIFU sonication. It can also be used by other institutions with the same clinical equipment. Increased Dox concentration (14.9±2.5 μg/g) was measured in the MRgHIFU-treated group compared to the Dox-only group (9.5±1.6 μg/g), indicating an approximate 60% increase with p=0.05. The results were consistent with the increased spatial drug distributions by fluorescence imaging. Histological analysis showed increased extravasation in MRgHIFU-treated prostate tumors suggesting increased drug delivery with MRgHIFU (3).

Based on these studies, we also explored the feasibility of pulsed high-intensity focused ultrasound (pHIFU) for non-thermal cancer therapy. The InSightec MRgHIFU system was used in this study to perform image-guided, non-thermal sonications (temperature < 40 °C, as measured by real-time MR thermometry). Nude mice with implanted (LNCaP) prostate cancers were treated with pHIFU (1MHz;

5&25W acoustic power, 0.1&0.5 duty cycle; 60sec duration). The animals were allowed to survive for 4 weeks after the treatment. The tumor growth was monitored on a 1.5T MR scanner and compared with the control group. Our results showed that **s**ignificant tumor growth delay was observed in the mice treated with pHIFU. The mean tumor volume for the pHIFU treated mice was 30% and 65% smaller than that of the control mice for 5W/0.5duty cycle and 25W/0.1duty cycle treatment settings, respectively.

Key Research Accomplishments

We have accomplished the following tasks:

- We performed experiments to characterize the output of the focused ultrasound unit using MR guidance.
- We performed phantom studies to determine the ultrasonic parameters including the frequency, acoustic power and exposure duration for in vivo MRgHIFU drug delivery studies.
- We developed techniques for prostate tumor implantation orthotopically.
- We developed MRgHIFU treatment techniques for small animals using a clinical MRgHIFU system (an InSightec ExAblate 2000 system and a GE 1.5 T MR scanner).
- We verified ultrasound treatment parameters derived from phantom studies using tumor bearing mice using Doxorubicin.
- We performed animal studies on determination of the uptake of AS-MDM2 in the MRgHIFU treated tumors.
- We performed studies on the determination of the uptake of AS-bcl2 in MRgHIFU treated tumors.
- We performed studies on the determination of the efficacy of AS-MDM2+MRgHIFU in inhibiting prostate tumor growth *in vivo*.
- We performed *in vivo* experiments to investigate the use of MRgFUS for the enhancement of chemotherapy agents in prostate tumors grown in nude mice using [3H]-docetaxel. We demonstrated that the [3H]-docetaxel concentration in tumors treated with MRgFUS was significantly increased compared with those without the MRgHIFU treatment.
- We performed studies on pulsed ultrasound treatment parameters and a set of ultrasound parameters has been established, which can be used by other institutions to study drug delivery with the same clinical MRgHIFU treatment system.
- We evaluated the drug enhancement in tumors for Dox by MRgHIFU using optimal ultrasound parameters.
- We performed experiments to investigate the effectiveness of the increased uptake of docetaxel by MRgHIFU in combination with RT in prostate tumor control *in vivo*.

Reportable Outcomes Resulting From or Supported in Part by this Grant / Bibliography of Publications

Peer-reviewed papers: (first and corresponding author)

1. **Chen L**, Mu Z, Hachem P, Ma C-M and Pollack A. MR-guided focused ultrasound: enhancement of intratumoral uptake of [^{3}H]-docetaxel *in vivo Phys. Med. Biol*., 55: 7399-7410 (2010)

2. Z Mu, C-M Ma, X Chen, A Pollack and **L Chen**. MR Guided Pulsed High Intensity Focused Ultrasound Enhancement of Docetaxel Combined with Radiotherapy for Prostate Cancer Treatment *Phys. Med. Biol*. **57** 535–545 (2012)
3. Xiaoming Chen, Dusica Cvetkovic, C-M Ma, **Lili Chen** Quantitative Study of Focused Ultrasound Enhanced Doxorubicin Delivery to Prostate Tumor *In Vivo* with MRI guidance *Med. Phys*. **39** 2780-2786 (2012)

Peer Reviewed Proceedings, Abstracts/ Presentations:

4. **L Chen**, Z Mu, P Hachem, C-M Ma, A Pollack. Enhancement of Drug Delivery in Prostate Tumor *in vivo* Using MR Guided Focused Ultrasound (MRgHIFU). WC, IFMBE Proceedings 25: pp341-344, 2009
5. **L Chen,** C Ma, T Richardson, G Freedman, A Konski. Treatment of Bone Metastasis Using MR Guided Focused Ultrasound. *Medical Physics*: 36: 2486, 2009.
6. **L Chen**, Z Mu, P Hachem, C-M Ma and A Pollack Enhancement of ^{3}H-Docetaxel Delivery in Prostate Tumor *in vivo* using MR Guided Focused Ultrasound (MRgHIFU) *Int J Rad Onc Biol Phys* 75(3) Supplement, S563, 2009
7. C Ma, **L Chen,** A Pollack, A Konski, G Freedman, M Buyyounouski. Quality Assurance for MR Guided Focused Ultrasound as a Multi-Modality Platform for Cancer Therapy. *Medical Physics*: 36: 2631, 2009
8. **L Chen**, Z Mu, P Hachem, C-M Ma, A Wallentine and A Pollack. Synergetic Effect of Docetaxel and MR Guided Focused Ultrasound (MRgFUS) for Prostate Cancer. *Medical Physics*: 37: 3133, 2010
9. **L Chen**, Z Mu, A Pollack and C Ma. An In Vivo Study On the Enhancement of Gene Therapy with MR-Guided Focused Ultrasound (MRgFUS). *Medical Physics*: 37: 3134, 2010
10. C Ma, Z Mu and **L Chen.** MR Guided High-Intensity Focused Ultrasound for Cancer Therapy; A Feasibility Study Using An Animal Model. *Medical Physics*: 37: 3456, 2010
11. C Ma, Z Mu and **L Chen.** Non-Thermal Cell Damage and Therapeutic Potential of MR Guided High-Intensity Focused Ultrasound. *Medical Physics*: 37: 3176, 2010
12. **L Chen**, Z Mu, X Chen, D Cvetkovic, A Pollack, and C-M Ma, MR guided pulsed high intensity focused ultrasound enhancement of chemotherapy for prostate cancer *Medical Physics*: 38: 3698, 2011
13. C-M Ma, D Cvetkovic, X Chen**,** L Chen. Non-thermal pulsed focused ultrasound for cancer therapy *Medical Physics*: 38: 3824, 2011
14. D Cvetkovic, X Chen**,** C Ma and **L Chen** *Histological changes in the mouse prostate tumors treated with non-thermal pulsed focused ultrasound Medical Physics*: 38: 3824, 2011
15. **L Chen**, Z Mu, X Chen, D Cvetkovic, A Pollack and C Ma Therapeutic effects of pulsed focused ultrasound enhancement of docetaxel combined with radiotherapy on prostate cancer in vivo *Medical Physics*: 38: 3825, 2011
16. X Chen, D Cvetkovic, C Ma and **L Chen** Enhanced uptake of doxorubicin in prostate tumor using pulsed focused ultrasound *Medical Physics*: 38: 3838, 2011
17. X Chen, D Cvetkovic, C Ma and **L Chen** Treatment assessment for pulsed focused ultrasound therapy of prostate tumor using a clinical 1.5 T MRI *Medical Physics*: 38: 3839, 2011
18. C-M Ma, D Cvetkovic, X Chen, Z Mu, **L Chen,** "Investigation of Non-Thermal Pulsed HIFU for Cancer Therapy", Proc. of International Society for Therapeutic Ultrasound Symposium, New York City, NY, 2011
19. **L Chen,** Z Mu, D Cvetkovic, X Chen, A Pollack, C-M Ma, "Enhancement of Docetaxel by Pulsed HIFU for Prostate Cancer Therapy - an In-Vivo Study", Proc. of International Society for Therapeutic Ultrasound Symposium, New York City, NY, 2011

20. X Chen, D Cvetkovic, C-M Ma, **L Chen,** "Pulsed-FUS Enhancement of Doxorubicin Uptake in Prostate Cancer", Proc. of International Society for Therapeutic Ultrasound Symposium, New York City, NY, 2011
21. **L Chen,** C Ma, T Richardson, G Freedman, A Konski, X Chen, J Fan, R Price, J Meyer Clinical Experience at Fox Chase Cancer Center for Treatment of Bone Metastases Using ExAblate 2000 with MR Guidance *Medical Physics*: 39: 4012, 2012
22. **L Chen,** N Rapoport, X Chen, D Cvetkovic, J Xue, q xu, X Tong, H Liu, R Gupta, C Ma Targeted Drug Delivery Technique Employing Pulsed Focused Ultrasound for Treatment of Prostate *Medical Physics*: 39: 3890, 2012
23. **L Chen,** High Intensity Focused Ultrasound (HIFU/FUS) in Cancer Therapy. World Congress on Medical Physics & Biomedical Engineering Beijing (invited talk) 2012
24. **L Chen**, XM Chen, D Cvetkovic, J Xue, XU Tong, Q Xu, R Gupta, N Rapoport , C-M Ma Targeted Drug Delivery Technique Using Pulsed Focused Ultrasound (pFUS) For Prostate Cancer Therapy. World Congress on Medical Physics & Biomedical Engineering Beijing, (oral presentation) 2012
25. **L Chen**, G Shan, W Hu, I Emam, Q Xu, J Li, B Proce and C Ma. Dosimetric evaluation of inter-factional motion for image-guided prostate IMRT ASTRO's 54th Annual Meeting, Boston, 2012
26. **L Chen,** C-M Ma, Terry Richardson, Gary Freedman, Andre Konski and Joshua Meyer. A Comprehensive Quality Assurance Program for Bone Palliation Using MR Guided Focused Ultrasound: Fox Chase Experience. Focused Ultrasound Focused Ultrasound Foundation, Symposium, Washington DC (oral) 2012
27. R Gupta, X Chen, D Cvetkovic, N Rapoport, C-M Ma and **L Chen** Development of Ultrasound Responsive- Docetaxel Encapsulated Perfluorocarbon Nanodroplets for Treatment of Prostate Cancer. *FUSF symposium*, Abstract 2012
28. D Cvetkovic, X Chen, C-M Ma, **L Chen. BEST IN PHYSICS (IMAGING**) - Evaluation of Apoptosis and Proliferation in Non-Thermal Pulsed HIFU Treated Mouse Prostate Tumors. *Medical Physics* 36:4003, (2012)
29. X Chen , D Cvetkovic, J Xue, **L Chen**, C-M Ma. **BEST IN PHYSICS (THERAPY)** - Combined Effects of Pulsed Non-Thermal Focused Ultrasound and Radiotherapy for Prostate Cancer Treatment. *Medical Physics* 36: 3899 (2012)
30. Ma C-M, Cvetkovic D, Chen XM, Gupta R and **Chen L** Non-Thermal Effect of Pulsed High-Intensity Focused Ultrasound – an in Vivo Study *FUSF symposium,* (2012).

Non peer-reviewed papers resulting from or supported in part by this grant: none

Funding applied for based on work resulting from or supported in part by this grant:

Title of the grant proposal: "MR Guided Pulsed Focused Ultrasound Mediated Targeted Chemotherapeutic-Agent Delivery in Multi-modality Management of Prostate Cancer**"**

Conclusions: Our study showed that drug uptake can be increased significantly by nonthermal HIFU. These results demonstrate the clinical potential of MRgHIFU-mediated drug delivery for prostate tumor treatment. By enhancing the local chemotherapeutic agent uptake in tumors, lower doses could be used to achieve the same treatment efficiency while significantly reducing its side effects, leading to improved quality of patient care. In addition, tumors exposed to pHIFU alone with similar parameters also showed significant tumor growth delay (14). As a result, pHIFU may not only enhance the local drug uptake but also cause additional tumor cell killing. These combined effects may provide a promising modality for prostate cancer therapy.

The effect of Gene therapy sing AS-MDM2 and bcl-2 is inconclusive even with the drug delivery enhancement as demonstrated by [3H]-docetaxel. Future studies are warranted using optimal MRgHIFU parameters and treatment regimens (and other gene drugs) to confirm our study results.

List of published papers quoted in the body of text:

1. **Chen L**, Mu Z, Hachem P, Ma C-M and Pollack A. MR-guided focused ultrasound: enhancement of intratumoral uptake of [^{3}H]-docetaxel *in vivo Phys. Med. Biol*., 55: 7399-7410 (2010)
2. Z Mu, C-M Ma, X Chen, A Pollack and **L Chen**. MR Guided Pulsed High Intensity Focused Ultrasound Enhancement of Docetaxel Combined with Radiotherapy for Prostate Cancer Treatment *Phys. Med. Biol*. **57** 535–545 (2012)
3. Xiaoming Chen, Dusica Cvetkovic, C-M Ma, **Lili Chen** Quantitative Study of Focused Ultrasound Enhanced Doxorubicin Delivery to Prostate Tumor *In Vivo* with MRI guidance *Med. Phys*. **39** 2780-2786 (2012)

References:

1. Chen L**,** Mu Z, Hachem P, Ma C-M and Pollack A. (2010) MR-guided focused ultrasound: enhancement of intratumoral uptake of [^{3}H]-docetaxel *in vivo* Phys. Med. Biol. 55: 7399-7410
2. Mu Z, Ma C-M, Chen X, Pollack A and Chen L. (2012) MR Guided Pulsed High Intensity Focused Ultrasound Enhancement of Docetaxel Combined with Radiotherapy for Prostate Cancer Treatment *Phys. Med. Biol*. 57 535–545
3. Xiaoming Chen, Dusica Cvetkovic, C-M Ma, **Lili Chen** Quantitative Study of Focused Ultrasound Enhanced Doxorubicin Delivery to Prostate Tumor *In Vivo* with MRI guidance *Med. Phys*. **39** 2780-2786 (2012)
4. Chen X, Cvetkovic D, Xue J, **Chen L**, Ma C-M. (2012) BEST IN PHYSICS (THERAPY) - Combined Effects of Pulsed Non-Thermal Focused Ultrasound and Radiotherapy for Prostate Cancer Treatment. *Medical Physics* 36: 3899, Abstract
5. Cvetkovic D, Chen X, Ma C-M, **Chen Lili** (2012) BEST IN PHYSICS (IMAGING) - Evaluation of Apoptosis and Proliferation in Non-Thermal Pulsed HIFU Treated Mouse Prostate Tumors. *Medical Physics* 36:4003, Abstract
6. 6.ter Haar G R, Daniels S and Morton K. Evidence of acoustic cavitation in vivo:thresholds for bubble formation with 0.75 MHz continuous wave and pulsed beams *IEEE Trans. Ultrasonics Ferroelectrics Freq. Control UFFC*-33 162-64, (1986)
7. Yuh EL, Shulman SG, Mehta SA, Xie J, Chen L, Frenkel V, Bednarski MD, Li K C. (2005) Delivery of systemic chemotherapeutic agent to tumors by using focused ultrasound: study in a murine model. *Radiology,* 234**,** 431-7
8. Stoyanova R, Hachem P, Hensley H, Khor LY, Mu Z, Hammond ME, Agrawal S, Pollack A. (2007) Antisense-MDM2 sensitizes LNCaP prostate cancer cells to androgen 3deprivation, radiation, and the combination in vivo. *Int J Radiat Oncol Biol Phys,* 68(4):1151-60
9. Wu F, Wang Z B, Chen W Z, Zhu H, Bai J, Zou J Z, Li K Q, Jin C B, Xie F L and Su H B 2004 Extracorporeal high intensity focused ultrasound ablation in the treatment of patients with large hepatocellular carcinoma *Annals of surgical oncology* **11** 1061-9
10. Banerjee S, Hussain M, Wang Z, Saliganan A, Che M, Bonfil D, Cher M and Sarkar F H 2007 In vitro and in vivo molecular evidence for better therapeutic efficacy of ABT-627 and taxotere combination in prostate cancer Cancer research 67 3818-26

11. Jones D R, Taylaor M D, Petroni G R et al 2010 Phase I trial of intrapleural docetaxel administered through an implantable catheter in subjects with a malignant pleural effusion. J Thorac Oncol 5 75-81
12. Spigel D R, Greco F A, Thompson D S et al 2010 Phase II study of cetuximab, docetaxel, and gemcitabine in patients with previously untreated advanced non-small-cell lung cancer. Clin Lung Cancer 11 198-203
13. Engels F K, Buijs D, Loos W J, Verweij J, Bakker W H and Krenning E P 2006 Quantification of [3H]docetaxel in feces and urine: development and validation of a combustion method Anti-cancer drugs 17 63-7
14. C-M Ma, D Cvetkovic, X Chen, L Chen. Non-thermal pulsed focused ultrasound for cancer therapy Medical Physics: 38: 3824, 2011

List of Personnel:

Lili Chen, Ph.D., Principal Investigator
Dusica Cvetkovic, M.D., Research Associate
Zhaomei Mu, M.D., Staff Scientist

Appendices:

Copies of two publications

1. Xiaoming Chen, Dusica Cvetkovic, C-M Ma, **Lili Chen** Quantitative Study of Focused Ultrasound Enhanced Doxorubicin Delivery to Prostate Tumor *In Vivo* with MRI guidance. *Med. Phys*. **39** 2780-2786 (2012)
2. Z Mu, C-M Ma, X Chen, A Pollack and **L Chen**. MR-Guided Pulsed High Intensity Focused Ultrasound Enhancement of Docetaxel Combined with Radiotherapy for Prostate Cancer Treatment. *Phys. Med. Biol*. **57** 535–545 (2012)

Copy of AAPM abstracts (2012) including 2 best papers selected this year by AAPM

1. **L Chen,** C Ma, T Richardson, G Freedman, A Konski, X Chen, J Fan, R Price, J Meyer Clinical Experience at Fox Chase Cancer Center for Treatment of Bone Metastases Using ExAblate 2000 with MR Guidance. *Medical Physics*: 39: 4012, 2012
2. **L Chen,** N Rapoport, X Chen, D Cvetkovic, J Xue, q xu, X Tong, H Liu, R Gupta, C Ma Targeted Drug Delivery Technique Employing Pulsed Focused Ultrasound for Treatment of Prostate. *Medical Physics*: 39: 3890, 2012
3. X Chen , D Cvetkovic, J Xue, **L Chen**, C-M Ma. **BEST IN PHYSICS (THERAPY)** - Combined Effects of Pulsed Non-Thermal Focused Ultrasound and Radiotherapy for Prostate Cancer Treatment. *Medical Physics* 36: 3899 (2012)
4. D Cvetkovic, X Chen, C-M Ma, **L Chen BEST IN PHYSICS (IMAGING**) - Evaluation of Apoptosis and Proliferation in Non-Thermal Pulsed HIFU Treated Mouse Prostate Tumors. *Medical Physics* 36:4003, (2012)

Quantitative study of focused ultrasound enhanced doxorubicin delivery to prostate tumor *in vivo* with MRI guidance

Xiaoming Chen, Dusica Cvetkovic, C.-M. Ma, and Lili Chen[a)]
Department of Radiation Oncology, Fox Chase Cancer Center, Philadelphia, Pennsylvania 19111

(Received 29 November 2011; revised 22 March 2012; accepted for publication 5 April 2012; published 24 April 2012)

Purpose: The purpose of this study was to investigate the potential of MR-guided pulsed focused ultrasound (pFUS) for the enhancement of drug uptake in prostate tumors *in vivo* using doxorubicin (Dox).
Methods: An antitumor drug Dox, an orthotopic animal prostate tumor model using human prostate cancer, LNCaP cell line, and a clinical FUS treatment system (InSightec ExAblate 2000) with a 1.5T GE MR scanner were used in this study. First, experiments on a tissue mimic phantom to determine the optimal acoustic power and exposure durations with a 10% duty cycle and a 1 Hz pulse rate were performed. The temperature variation was monitored using real-time MR thermometry. Second, tumor-bearing animals were treated with pFUS. There were three groups ($n = 8$/group): group 1 received pFUS + Dox (10 mg/kg i.v. injection immediately after pFUS exposure), group 2 received Dox only (10 mg/kg i.v. injection), and group 3 was a control. Animals were euthanized 2 h after the pFUS treatment. The Dox concentration in the treated tumors was measured by quantifying fluorescent tracers using a fluorometer. Third, the histological changes of tumors with and without pFUS treatments were evaluated. Finally, experiments were performed to study the spatial drug distribution in tumors after the pFUS treatment, in which two animals received pFUS + Dox, two animals received Dox only, and one animal was used as control. Two hours following the treatment, animals were euthanized and processed. The Dox distribution was determined using a fluorescence microscope.
Results: Parametric measurements using a tissue phantom showed that the temperature increased with an increasing acoustic power (from 10 to 50 W) or sonication duration (from 10 to 60 s) with a given acoustic frequency of 1 MHz, duty cycle 10%, and pulse rate 1 Hz. A set of ultrasound parameters was identified with which the temperature elevation was less than 5 °C, which was used for nonthermal pFUS sonication. Increased Dox concentration (14.9 ± 2.5 μg/g) was measured in the pFUS-treated group compared to the Dox-only group (9.5 ± 1.6 μg/g), indicating an approximate 60% increase with $p = 0.05$. The results were consistent with the increased spatial drug distributions by fluorescence imaging. Histological analysis showed increased extravasation in pFUS-treated prostate tumors suggesting increased drug delivery with pFUS.
Conclusions: The results showed that pFUS-enhanced drug uptake in prostate tumors was significant. This increased uptake may be due to increased extravasation by pFUS. Optimal pFUS parameters may exist to maximize the drug uptake, and this study using Dox demonstrated a quantitative method for such systematic parametric studies. In addition, this study may provide useful data for the potential application of pFUS-mediated Dox delivery for prostate tumor therapy. [http://dx.doi.org/10.1118/1.4705346]

Key words: doxorubicin, focused ultrasound, HIFU, prostate cancer

I. INTRODUCTION

Pulsed high-intensity focused ultrasound (pFUS) is able to create acoustic cavitation (microbubbles) in the focused region of tissues. It has been suggested that these microbubbles can increase the permeability of the local vascular wall and cell membrane.[1–3] It is also suggested that radiation force may induce local tissue dilation and thus widen the interstitial space to enhance the interstitial transport.[3,4] Conventionally used for thermal ablation, high-intensity focused ultrasound was recently explored as a technique to enhance local drug delivery to tissues by using the pulse mode with low acoustic powers and duty cycles, which will maintain an insignificant local temperature elevation thus avoiding thermal damage. For simplicity, the term "nonthermal" is used in this work to refer to this safe temperature working zone of pFUS in contrast to thermal ablation. With pFUS, energy is delivered and focused to the treatment target by ultrasound waves without invasion to normal tissues. With the guidance of magnetic resonance imaging or diagnostic ultrasound, accurate targeting can be achieved. Previous experiments on small animals have demonstrated that focused ultrasound exposure can enhance the delivery of different agents into tumors[4–8] or disrupt the local blood–brain barrier in a reversible way.[9,10] For example, Dromi *et al.*[6] used pFUS-induced mild temperature elevation (4–5 °C) to trigger Dox-loaded low-temperature-sensitive liposomes and thus enhance the delivery of doxorubicin (Dox) in a

mouse mammary tumor model. Hancock *et al.*[4] showed the enhanced delivery of a variety of fluorophores in the calf muscle of mice when combined with pFUS exposure, while Hynynen *et al.*[9] investigated the local and reversible blood–brain barrier disruption by noninvasive pFUS and looked at the suitable acoustic parameters for trans-skull sonications.

These preliminary studies used custom ultrasound devices that were tested in different animal tumor models. Although the results are promising, the translation of these techniques to clinical application requires extensive studies. Detailed studies are still necessary to examine the potential clinical applications of pFUS on other drugs and tumor types. Investigations of optimal pFUS parameters are also critical in order to maximize the enhancement of therapeutic agent uptake in treated tumor volumes. Developing quantitative methods to evaluate the pFUS enhancement would be necessary for such a systematic parametric study. Furthermore, MRI can be used for tumor delineation, treatment planning, and ultrasound beam placement with 1 mm accuracy. MRI is also used to monitor the therapeutic effects of pFUS in real time by monitoring the temperature changes using MR thermometry. The MR-guided pFUS technique is increasingly accepted and has been integrated in several clinical FUS systems such as ExAblate 2000 (InSightec Ltd., Tirat Carmel, Israel) and Sonalleve (Philips Healthcare, Andover, MA). Animal studies with these clinical devices would be useful to facilitate future preclinical evaluations.

In this study, Dox was delivered to prostate tumors with the aid of MR-guided pFUS. Dox has been chosen for this study as it inherits fluorescent substance that allows us to evaluate the effects of the pFUS treatment by measuring the drug concentration in the treated tumor volume quantitatively using a fluorometer,[11] and the spatial drug distribution can be viewed by fluorescent imaging. In addition, it is an anthracycline antibiotic used for treatment of a wide spectrum of malignancies including prostate cancers. Clinical trails of Dox are being conducted for prostate cancers, especially for hormone refractory diseases.[12–14] However, the effectiveness of Dox is limited due to its high toxicity and side effects such as alopecia, acute nausea, vomiting, stomatitis, and suppression of bone marrow.[15–17] Accumulative uptake by the heart may cause cardiotoxicity and heart failure.[16] Repeated administration may also lead to strong multidrug resistance response in tumor cells.[18] To reduce its toxicity and side effects, new strategies were proposed to reduce the normal tissue uptake or offset the side effects of Dox. For example, Dox was encapsulated in the liposome to prolong the circulation time, reduce normal tissue uptake, and enhance accumulation in tumors.[14,19] Treatment regimens combining Dox with other drugs such as sildenafil was also investigated to offset the side effects of Dox.[15] From a drug delivery viewpoint, enhancing the local uptake of Dox in prostate tumors would reduce the total dose needed for the same therapeutic efficacy and, therefore, reduce the toxicity and side effects.

The purpose of this study was to quantitatively investigate the effect of MR-guided pFUS on the uptake of Dox in prostate tumors *in vivo*. An orthotopic animal prostate tumor model was developed using a human LNCaP tumor cell line to best mimic a clinical scenario. A clinical FUS system, Insightec ExAblate 2000, which received FDA clearance for the treatment of uterine fibroids, was used with a 1.5T GE MR scanner for MR-guided pFUS treatment. We hypothesized that the enhancement of intratumoral uptake of Dox may improve tumor growth inhibition without increasing systemic toxicity or using lower doses to achieve the same treatment efficacy with reduced systemic side effects. This quantitative study will test the method for a future systemic parametric study to maximally enhance the tumor uptake. The results may also provide important preclinical data for the use of pFUS as a modality to enhance drug delivery for the treatment of prostate cancers.

II. MATERIALS AND METHODS

II.A. Study of the pFUS treatment parameters

In order to avoid potential thermal damage, a tissue phantom study was conducted to evaluate the pFUS-induced temperature elevation with various acoustic power and sonication duration. An approximately cylindrical tissue phantom (diameter = ~10 cm, length = ~13 cm) provided by the vendor (InSightec Ltd., Tirat Carmel, Israel) was used. The experiment setup was similar to the animal experiment described below (Fig. 1) except that a larger surface coil

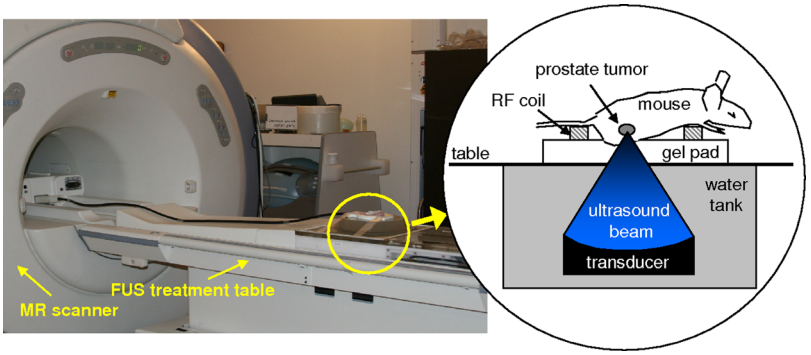

FIG. 1. Experimental setup for MR-guided pFUS exposure of prostate tumors in mice. The setup includes an MR scanner, pFUS treatment table, an acoustic gel pad, and a small RF surface coil. The mouse was in a prone position and the ultrasound beam was delivered from below. A small tissue phantom was also placed next to the mouse to verify the accuracy of the focal ultrasound delivery before treatment.

(diameter = ~15 cm) and a tissue phantom were used. The tissue phantom was manufactured by ATS Labs, Inc. (Bridgeport, CT) with acoustic properties similar to those of human soft tissue (the attenuation coefficient = 0.503 dB cm^{-1} MHz^{-1}; speed of sound = 1538 MPS; estimated specific heat = 2.684 cal/g). With the given duty cycle of 10%, pulse rate 1 Hz, and acoustic frequency 1 MHz, the phantom was sonicated with various acoustic powers ranging from 10 to 50 W and sonication durations ranging from 10 to 60 s in 10 W and 10 s increments, respectively. The temperature elevations in the focal zone were measured for each pair of parameters (i.e., acoustic power and sonication duration) using MR thermometry, which is a machine built-in software function. The relation of the temperature elevation to acoustic power and exposure duration was plotted by bilinearly interpolating the measured data.

II.B. Orthotopic prostate tumor model

An animal prostate tumor model was developed by implanting human prostate cancer LNCaP cells in the prostates of nude mice. The cells were obtained from the American Type Culture Collection (ATCC) and cultured in Dulbecco's modified Eagle's medium (DMEM)-F12 medium, containing 10% fetal bovine serum (FBS), 1% L-glutamine, and 1% penicillin–streptomycin as described previously.[8,20] Male athymic Balb/c nude mice (6 weeks old) were purchased from Harlan (Indianapolis, IN). Animal studies were carried out in compliance with a protocol approved by the Institutional Animal Care and Use Committee (IACUC) of Fox Chase Cancer Center (FCCC). Aseptic techniques were used for injection of LNCaP cells in the prostates of nude mice as described previously.[8] Nude mice were anesthetized using methoxyflurane. A lower midline incision was made above the presumed location of the bladder. The dorsal prostate lobes were exposed and 1×10^6 LNCaP cells in 25 μl volume were injected with a 30-gauge needle. The incision was sealed by suturing the muscle layer and using two–three wound clips for the skin layer. Buprenorphine was given immediately after the tumor implantation for pain relief.

II.C. MR-guided pFUS exposure

The prostate tumor volume was monitored weekly after tumor implantation using a 1.5T GE MR scanner (GE Healthcare, Waukesha, WI). Animals were anesthetized for MR scanning with an intramuscular (i.m.) injection of a mixed solution of ketamine (60 mg/kg) and acepromazine (2.5 mg/kg) in 15 μl volume. A 15-min anesthesia was required to immobilize the animal during MR scanning. When the prostate tumor volume reached approximately 100 mm^3, treatment was initiated. Tumor-bearing mice were randomly assigned to one of the three experimental groups ($n = 8$/group): (1) Dox following pFUS exposure (pFUS + DOX group), (2) Dox only (DOX group), and (3) a control group. MR-guided pFUS treatment was performed using the ExAblate 2000 (InSightec Ltd., Tirat Carmel, Israel) with a 1.5T GE MR scanner. Figure 1 shows the experimental setup. Animals were anesthetized for the pFUS treatment with ketamine and acepromazine in 30 μl volume i.m. and placed on an acoustic gel pad, which was laid on the FUS treatment table. Caution was taken to ensure that the mouse, the acoustic gel, and the treatment table were well coupled acoustically to avoid the formation of air bubbles. A ring-shaped surface coil (diameter = ~8 cm) was used for the MR signal detection. T2-weighted MR images were acquired using a fast-recovery fast spin-echo (FRFSE) sequence with parameters: TR/TE = 2200/85 ms, NEX = 3, matrix = 288 × 288, FOV = 7 × 7 cm^2 (resolution = 0.243 × 0.243 mm^2), and slice thickness = 2 mm. Both coronal and axial scans were performed and the acquired MR images were loaded immediately into the FUS treatment planning system for treatment planning (Fig. 2).

Nonthermal sonications were delivered by keeping the body temperature below 42 °C. The body temperature during sonication was monitored in real time (~3 s delay) by MR thermometry using a temperature-induced proton resonance frequency shift method. MR thermometry scans were acquired using a fast spoiled gradient echo (FSGR) sequence with parameters: TR/TE = 25.9/12.8 ms, flip angle = 30°, NEX = 1, number of echo = 1, FOV = 22 × 22 cm^2, matrix = 256 × 128, and slice thickness = 3 mm. Tumor-bearing mice from group 1 were exposed to pFUS using the following parameters: 1 MHz ultrasound, 25 W acoustic power, and 1 Hz pulse rate with a 10% duty cycle for 60 s for each sonication spot. During the pFUS treatment, temperature elevations between 4 and 5 °C were observed under these pFUS parameters. The focal length was 98–102 mm and the aperture of pFUS transducer was 12 cm. The ultrasound focal zone is an elongated ellipsoid with a longitudinal length of 6.8 mm (−3 dB) and a radial diameter of 1.25 mm (−3 dB). The estimated peak-negative pressure in the focal zone was 7.8 MPa and the average acoustic intensity was 20.4 W/mm^2. A total of four–eight sonication spots were used to cover the entire tumor volume depending on the tumor size. The pFUS parameters were selected based on our tissue phantom study. Tail vein injections (volume of 100 μl) of Dox (10 mg/kg) were given to mice in group 1 immediately after pFUS exposure (within 10 min). Group 2 received the same Dox injection, but without pFUS exposure. No Dox injection was given to the control animals.

II.D. Assay for intratumoral doxorubicin content

Mice were euthanized 2 h after the Dox injection assuming the drug had circulated into the prostate tumor. Prostate tumors were excised, weighed, and homogenized in Eppendorf 1.5 ml tubes. A lysis buffer (800 μl) containing 3% hydrochloride, 48.5% ethanol, and 48.5% double-distilled water was added to tissue homogenates, vortexed, and stored in the dark at 4 °C overnight. The next day the lysates were centrifuged at 5000 rpm for 10 min at 4 °C and supernatants were collected. Three 100 μl supernatant aliquots from each sample were placed in 96-well plates and read with a Fluoroskan Ascent microplate fluorometer and luminometer (excitation at 485 nm; emission at 538 nm; Thermo Fisher Scientific, Waltham, MA). Fluorescence readings were compared with values from a standard calibration curve. The

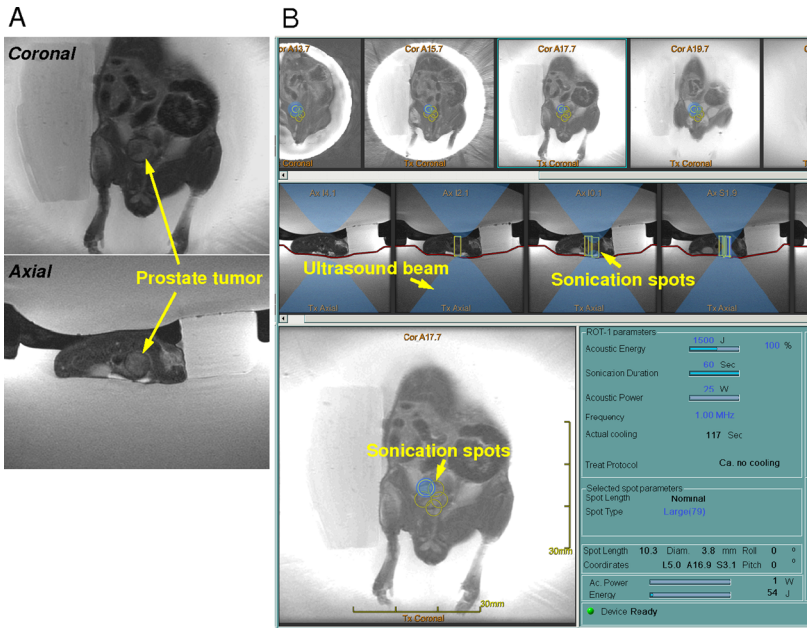

FIG. 2. (a) MR coronal and axial views of a typical mouse prostate tumor for pFUS treatment. (b) Real-time treatment planning based on acquired MR images (top: coronal view of sonication spot distribution; middle: axial view of ultrasound beam passing through the tumor and the surrounding materials; bottom: a zoomed coronal view of sonication spots covering the mouse prostate tumor). Planned sonication spots had a cylindrical shape with a diameter of 3.8 mm and a length of 10.3 mm.

calibration curve comprised serial dilutions of Dox and related the fluorescence readings to the Dox mass [Fig. 4(a)]. The total amount of Dox in each tumor sample was normalized to its weight and expressed as microgram of Dox per gram of tumor weight. Fluorescence values of the control samples were subtracted as background.

II.E. Light and fluorescence microscopy analysis

A separate experiment was conducted to compare the Dox distribution in the tumor tissue with and without pFUS treatment using fluorescence microscopy. Five tumor-bearing mice were used for this experiment; two received pFUS and Dox as described above, and two received Dox only. One animal received no treatment and was used for determination of the background levels of fluorescence in the tissue. Two hours following the treatment, animals were euthanized, tumors were harvested, snap frozen in liquid nitrogen, and cut into frozen sections using Leica CM1850 cryostat (Leica Microsystems GmbH, Wetzlar, Germany). Tumor sections were examined using the Eclipse600 microscope (Nikon Instruments, Inc., Melville, NY) to determine the difference of the spatial Dox distribution among various groups.

An additional experiment was conducted to compare histological changes between pFUS-treated prostate tumors ($n = 3$) and control, untreated tumors ($n = 3$) using light microscopy. Tumor-bearing mice were given the same pFUS exposures as described above and euthanized within 30 min of treatment. Prostate tumors were removed, fixed in 10% neutral buffered formalin, and embedded in paraffin. Paraffin blocks were used to generate the hematoxylin and eosin (H&E)-stained sections. Slides were examined using a light microscope (Nikon) to observe histological changes after pFUS treatment.

II.F. Statistical analysis

Measured tumor Dox concentrations were analyzed statistically. The mean and standard deviation of the mean (SEM) were calculated and the results were expressed as *mean* ± *SEM*. To determine if there was a significant difference between treated and control groups, Student's *t*-test was used and a p-value ≤ 0.05 was considered to be significant.

III. RESULTS

III.A. pFUS-induced temperature elevation

Figure 3 shows the pFUS-induced temperature elevation based on the tissue phantom study using our experimental pFUS system (at acoustic frequency 1 MHz, duty cycle 10%, and pulse rate 1 Hz). Assuming that biological tissues are not damaged below 42 °C, Fig. 3 suggested that at 25 W acoustic power the exposure duration of 60 s would be safe to avoid tissue damage (assuming a normal body temperature of 37 °C and a <5 °C temperature elevation). It can be seen that the temperature increases exponentially with the acoustic power and the acoustic power and sonication duration follow an inverse relationship. When delivering the same acoustic energy at a lower acoustic power, a lower temperature increase was observed due to heat loss.

III.B. Quantitative measurement of Dox uptake in prostate tumor

Comparison of the Dox concentration in prostate tumors between mice treated with pFUS (pFUS + DOX) and without (DOX alone) showed a significant increase in Dox uptake in treated tumors (Fig. 4). Dox concentration in the pFUS-treated group was 14.9 ± 2.5 μg/g, while in the Dox only group it was 9.5 ± 1.6 μg/g. The difference between these two groups was statistically significant ($p = 0.05$). There was an approximately 60% increase of Dox uptake in the prostate tumors exposed to pFUS with the parameters used in this study. These results were consistent with our previous studies on Docetaxel.[8]

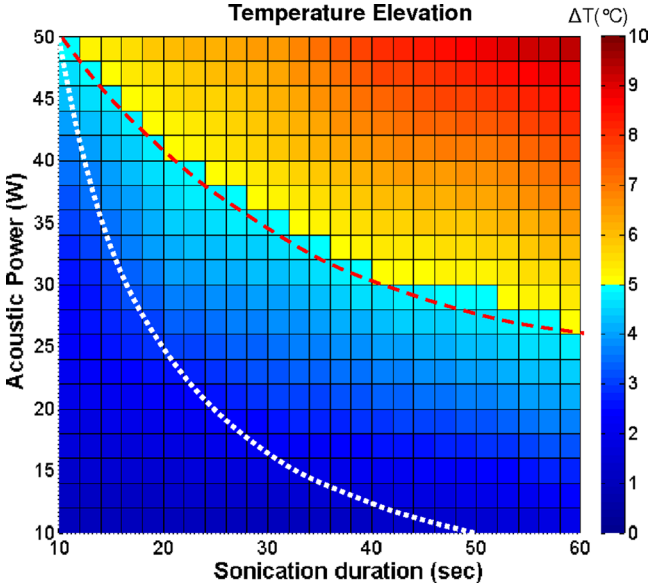

FIG. 3. pFUS-induced temperature elevation using different acoustic powers and sonication durations based on the tissue phantom measurement (acoustic frequency: 1 MHz; duty cycle: 10%; pulse rate: 1 Hz). The red dashed line indicates a 5 °C temperature elevation, which will increase the body temperature to 42 °C, assuming a normal body temperature of 37 °C. The white dotted line indicates the same acoustic energy delivered using different acoustic power and the temperature elevation changes.

III.C. Spatial Dox distribution in prostate tumor

The enhancement of Dox uptake in pFUS-treated tumors was confirmed by fluorescence microscopy. Figure 5 shows typical fluorescence micrographs of prostate tumor tissues from the three different groups, i.e., control, Dox injection only, and Dox injection after pFUS treatment. More Dox signals (emission from Dox) were observed in pFUS-treated tumor tissues compared to those without pFUS treatment. Images also show the inhomogeneous distribution of Dox in prostate tumor tissues. The observed distribution was consistent with findings of enhanced Dox uptake quantitatively measured using the fluorescence technique (Fig. 4).

III.D. Histology analysis

Figure 6 shows histological changes in prostate tumors with and without pFUS treatment. A significant increase in the blood cell extravasation was observed in the pFUS-treated tumors compared with those without the pFUS treatment. There were no implosion cysts[21] observed in the tumor tissues, indicating that no thermal damage occurred as was observed in thermal ablation. The increase in the blood extravasations demonstrated the increased permeability of blood vessels in the tumor tissues. Other histological changes such as extracellular matrix disintegration or increased intracellular spacing were not clearly evident.

IV. DISCUSSION

Previous studies by other groups have demonstrated that pulsed focused ultrasound can enhance local drug uptake in tumors. These preliminary studies used either a custom-made ultrasound device or different animal models.[4–7,22] Detailed studies are necessary to investigate the potential clinical applications of pFUS for individual drugs and tumor types. For example, drug transport into tumor tissues is affected by several factors, including agent permeability across the blood vasculature and microenvironment difference between various types of tumors, such as interstitial fluid pressure and tumor cell density.[23] On the other hand, tumor microenvironment changes induced by pFUS are most likely related to the treatment parameters used and also related to physical properties of the tumor itself. In this study, we quantitatively investigated the doxorubicin uptake in the prostate tumor with the aid of MR-guided pFUS. The orthotopically implanted mouse prostate tumor model was used to best mimic a clinical scenario. A commercially available clinical MR-guided pFUS system was used, which is currently under investigation for its clinical use for pFUS-

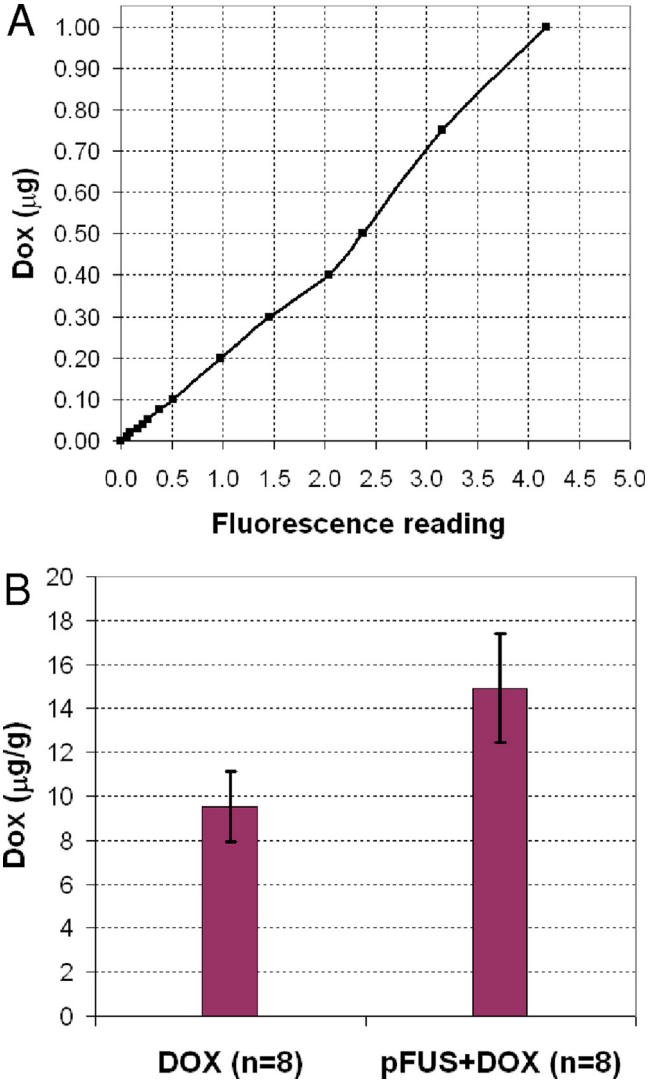

FIG. 4. (a) The doxorubicin fluorescence calibration curve showing the fluorescence readings for different mass of Dox. (b) Comparison of tumor Dox concentration between untreated (DOX) and pFUS-treated groups (pFUS + DOX). Tumor Dox concentration is defined as microgram of Dox per gram of tumor weight. In the pFUS + DOX group, it was 14.9 ± 2.5 μg/g, while in the DOX-only group it was 9.5 ± 1.6 μg/g ($p = 0.05$).

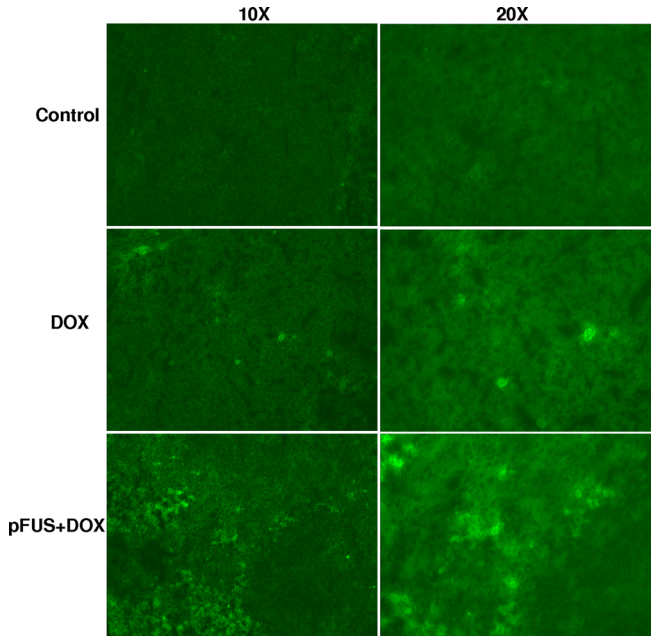

FIG. 5. Fluorescence photomicrographs of the Dox distribution in prostate tumors for different groups (control, DOX: Dox injection only; pFUS + DOX: Dox injection after pFUS treatment). Images were acquired with a magnification of 10× (left column) and 20× (right column).

enhanced drug delivery. Our study showed that pFUS exposures significantly enhanced the uptake of Dox in prostate tumors with increased blood extravasation.

The interactions between pFUS and tissues lead to several effects including mild temperature elevation due to local energy absorption, cavitation due to sufficiently low fluid pressure, and tissue strain due to radiation force. Previous mechanistic studies of pFUS enhancing effects suggested that the temperature elevation has no significant contribution to the delivery enhancement.[24] Instead, it is more likely due to the cavitation and radiation force that induce changes of local tissue properties such as increased vascular permeability and interstitial transport. In murine calf muscle exposed to pFUS, cavitation was detected using an *in vivo* monitoring technique.[24] Enlarged gaps between mice muscle fibers exposed to pFUS were clearly observed immediately or even 24 or 48 h after the pFUS treatment.[4] Extravasation was evident in several previous pFUS enhancement studies[4,7,24] as well as in this study. From a biomechanics viewpoint, the acoustic intensity or pressure applied on the tissue plays a major role in cavitation and radiation force and may directly determine the types of bioeffects. Previous pFUS studies have used various acoustic intensities ranging from ~2.2,[8] ~11.1,[7] ~13.7,[6,7,25] to ~26.6 W/mm^2 (Refs. 4, 24, and 26) for different tissues such as tumors and muscle. While different levels of pFUS enhancing effects were observed, it is not clear which acoustic intensity will give the maximal enhancement. A systematic parametric study using different acoustic intensities would be necessary in future studies.

Practically, several issues must be investigated for the use of pFUS as a modality to mediate the drug delivery to tumors, such as the acoustic power, focal spot temperature, and time point of drug injection. The temperature elevation at the focal spot is affected by several factors including the energy input rate, temperature gradient to surrounding region, and thermal transfer coefficient of the material. Increasing the energy input rate will increase temperature of the focal zone while a large temperature gradient and thermal transfer coefficient will increase the thermal flux out of the focal zone and decrease the temperature. The balance between the acoustic power and the heat loss in the focal zone determines the temperature elevation. As a result, higher temperature elevation was observed when using higher acoustic power, even though the total energy delivered did not change as seen in Fig. 3. In addition, a higher acoustic power of 25 W was used to enhance the Dox uptake in tumor which has an estimated peak-negative pressure of 7.8 MPa in the focal zone. Increasing the acoustic power will increase the pressure at the focal zone, which may finally lead to increased interstitial space and vessel wall opening and enhance drug uptake in tumors. However, in order to keep the final body temperature at a safe level, the option to increase power is limited due to the increased temperature as shown in Fig. 3. Higher pressure also has a tendency to induce other effects such as eruption of microbubbles.[1] The time point of drug injection may also play an important role in optimal drug delivery enhancement. In this study, drug was injected i.v. immediately after the pFUS exposure. For clinical applications, this could be done simultaneously with the pFUS exposure or at different time points to achieve a better uptake.

The results from this study are consistent with our previous study of enhanced [^{3}H]-docetaxel uptake in prostate tumors, where a lower acoustic power (4 W), higher duty cycle (50%), and pulse rate (5 Hz) were used for pFUS treatment with the same clinical MR-guided FUS system.[8] While the drug transport properties might differ between Dox and Docetaxel, enhanced uptake was observed in both studies with different data analysis tools. In this study, Dox was used for quantitative study by taking advantage of its fluorescence properties. Dox

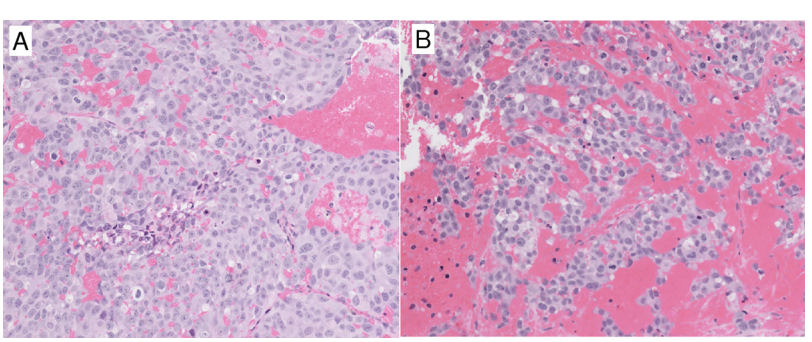

FIG. 6. H&E staining of mouse prostate tumor without pFUS treatment (a) and with pFUS treatment (b) (×20). Note the increased extravasation of blood cells in the pFUS-treated tumor.

also has a relatively long circulation time which allows sufficient plasma Dox concentration for the delivery enhancement study. According to the previous studies on humans and mice,[19,27,28] the terminal half-life of Dox was approximately 25–30 h. The level of pFUS enhancing effects may be determined by pFUS parameters. Specific pFUS parameters may exist to maximize the drug uptake enhancement, and further studies are needed to investigate such optimal pFUS parameters for maximal Dox uptake. This study provides a quantitative method for such systematic studies.

This study showed that Dox uptake in prostate tumors can be enhanced significantly by nonthermal pFUS. These results demonstrate the clinical potential of pFUS-mediated drug delivery for prostate tumor treatment. By enhancing the local Dox uptake in tumors, lower doses could be used to achieve the same treatment efficiency while significantly reducing its side effects, leading to improved quality of patient care. In addition, tumors exposed to pFUS with similar parameters also showed significant tumor growth delay.[29] As a result, pFUS may not only enhance the local drug uptake but also cause additional tumor cell killing. These combined effects may provide a promising modality for prostate cancer therapy. Future studies should be designed to investigate the optimal pFUS parameters and treatment regimens to achieve the maximal therapeutic effect.

ACKNOWLEDGMENTS

This study was supported by Focused Ultrasound Surgery Foundation and DOD PC073127. The authors would like to thank InSightec, Inc., for the technical support and Dr. Vladimir Kolenko and Dr. Konstantin Golovine at Fox Chase Cancer Center for sharing the fluorescence microscope and providing technical help.

[a]Author to whom correspondence should be addressed. Electronic mail: lili.chen@fccc.edu; Telephone: 215-728-3003; Fax: 215-728-4789.

[1]C. C. Coussios and R. A. Roy, "Applications of acoustics and cavitation to noninvasive therapy and drug delivery," Annu. Rev. Fluid Mech. **40**, 395–420 (2008).
[2]J. E. Kennedy, "High-intensity focused ultrasound in the treatment of solid tumours," Nat. Rev. Cancer **5**, 321–327 (2005).
[3]V. Frenkel, "Ultrasound mediated delivery of drugs and genes to solid tumors," Adv. Drug Delivery Rev. **60**, 1193–1208 (2008).
[4]H. A. Hancock, L. H. Smith, J. Cuesta, A. K. Durrani, M. Angstadt, M. L. Palmeri, E. Kimmel, and V. Frenkel, "Investigations into pulsed high-intensity focused ultrasound-enhanced delivery: Preliminary evidence for a novel mechanism," Ultrasound Med. Biol. **35**, 1722–1736 (2009).
[5]V. Frenkel, A. Etherington, M. Greene, J. Quijano, J. W. Xie, F. Hunter, S. Dromi, and K. C. P. Li, "Delivery of liposomal doxorubicin (Doxil) in a breast cancer tumor model: Investigation of potential enhancement by pulsed-high intensity focused ultrasound exposure," Acad. Radiol. **13**, 469–479 (2006).
[6]S. Dromi, V. Frenkel, A. Luk, B. Traughber, M. Angstadt, M. Bur, J. Poff, J. W. Xie, S. K. Libutti, K. C. P. Li, and B. J. Wood, "Pulsed-high intensity focused ultrasound and low temperature sensitive liposomes for enhanced targeted drug delivery and antitumor effect," Clin. Cancer Res. **13**, 2722–2727 (2007).
[7]E. L. Yuh, S. G. Shulman, S. A. Mehta, J. W. Xie, L. L. Chen, V. Frenkel, M. D. Bednarski, and K. C. P. Li, "Delivery of systemic chemotherapeutic agent to tumors by using focused ultrasound: Study in a murine model," Radiology **234**, 431–437 (2005).
[8]L. L. Chen, Z. M. Mu, P. Hachem, C. M. Ma, A. Wallentine, and A. Pollack, "MR-guided focused ultrasound: Enhancement of intratumoral uptake of H-3-docetaxel *in vivo*," Phys. Med. Biol. **55**, 7399–7410 (2010).
[9]K. Hynynen, N. McDannold, N. A. Sheikov, F. A. Jolesz, and N. Vykhodtseva, "Local and reversible blood-brain barrier disruption by noninvasive focused ultrasound at frequencies suitable for trans-skull sonications," Neuroimage **24**, 12–20 (2005).
[10]L. H. Treat, N. McDannold, N. Vykhodtseva, Y. Z. Zhang, K. Tam, and K. Hynynen, "Targeted delivery of doxorubicin to the rat brain at therapeutic levels using MRI-guided focused ultrasound," Int. J. Cancer **121**, 901–907 (2007).
[11]M. Gigli, S. M. Doglia, J. M. Millot, L. Valentini, and M. Manfait, "Quantitative study of doxorubicin in living cell-nuclei by microspectrofluorometry," Biochim. Biophys. Acta **950**, 13–20 (1988).
[12]R. Petrioli, A. I. Fiaschi, E. Francini, A. Pascucci, and G. Francini, "The role of doxorubicin and epirubicin in the treatment of patients with metastatic hormone-refractory prostate cancer," Cancer Treat Rev. **34**, 710–718 (2008).
[13]A. Heidenreich, F. Sommer, C. H. Ohimann, A. J. Schrader, P. Olbert, J. Goecke, and U. H. Engelmann, "Prospective randomized phase II trial of pegylated doxorubicin in the management of symptomatic hormone-refractory prostate carcinoma," Cancer **101**, 948–956 (2004).
[14]K. A. Harris, E. Harney, and E. J. Small, "Liposomal doxorubicin for the treatment of hormone-refractory prostate cancer," Clin. Prostate Cancer **1**, 37–41 (2002).
[15]A. Das, D. Durrant, C. Mitchell, E. Mayton, N. N. Hoke, F. N. Salloum, M. A. Park, I. Qureshi, R. Lee, P. Dent, and R. C. Kukreja, "Sildenafil increases chemotherapeutic efficacy of doxorubicin in prostate cancer and ameliorates cardiac dysfunction," Proc. Natl. Acad. Sci. U.S.A. **107**, 18202–18207 (2010).
[16]P. Singal, T. M. Li, D. Kumar, I. Danelisen, and N. Iliskovic, "Adriamycin-induced heart failure: Mechanisms and modulation," Mol. Cell. Biochem. **207**, 77–86 (2000).
[17]E. Rivera, "Liposomal anthracyclines in metastatic breast cancer: Clinical update," Oncologist **8**, 3–9 (2003).
[18]F. Shen, S. Chu, A. K. Bence, B. Bailey, X. Xue, P. A. Erickson, M. H. Montrose, W. T. Beck, and L. C. Erickson, "Quantitation of doxorubicin uptake, efflux, and modulation of multidrug resistance (MDR) in MDR human cancer cells," J. Pharmacol. Exp. Ther. **324**, 95–102 (2008).
[19]A. Gabizon, R. Catane, B. Uziely, B. Kaufman, T. Safra, R. Cohen, F. Martin, A. Huang, and Y. Barenholz, "Prolonged circulation time and enhanced accumulation in malignant exudates of doxorubicin encapsulated in polyethylene-glycol coated liposomes," Cancer Res. **54**, 987–992 (1994).
[20]Z. Mu, P. Hachem, H. Hensley, R. Stoyanova, H. W. Kwon, A. L. Hanlon, S. Agrawal, and A. Pollack, "Antisense MDM2 enhances the response of androgen insensitive human prostate cancer cells to androgen deprivation *in vitro* and *in vivo*," Prostate **68**, 599–609 (2008).
[21]L. L. Chen, I. Rivens, G. Terhaar, S. Riddler, C. R. Hill, and J. P. M. Bensted, "Histological-changes in rat-liver tumors treated with high-intensity focused ultrasound," Ultrasound Med. Biol. **19**, 67–74 (1993).
[22]K. Hynynen, "Focused ultrasound for blood-brain disruption and delivery of therapeutic molecules into the brain," Expert Opin. Drug Deliv. **4**, 27–35 (2007).
[23]R. K. Jain, "Delivery of molecular and cellular medicine to solid tumors," J. Controlled Release **53**, 49–67 (1998).
[24]B. E. O'Neill, H. Vo, M. Angstadt, K. P. C. Li, T. Quinn, and V. Frenkel, "Pulsed high intensity focused ultrasound mediated nanoparticle delivery: Mechanisms and efficacy in murine muscle," Ultrasound Med. Biol. **35**, 416–424 (2009).
[25]K. M. Dittmar, J. W. Xie, F. Hunter, C. Trimble, M. Bur, V. Frenkel, and K. C. P. Li, "Pulsed high-intensity focused ultrasound enhances systemic administration of naked DNA in squamous cell carcinoma model: Initial experience," Radiology **235**, 541–546 (2005).
[26]A. Khaibullina, B. S. Jang, H. Sun, N. Lee, S. Yu, V. Frenkel, J. A. Carrasquillo, I. Pastan, K. C. P. Li, and C. H. Paik, "Pulsed high-intensity focused ultrasound enhances uptake of radiolabeled monoclonal antibody to human epidermoid tumor in nude mice," J. Nucl. Med. **49**, 295–302 (2008).
[27]R. F. Greene, J. M. Collins, J. F. Jenkins, J. L. Speyer, and C. E. Myers, "Plasma pharmacokinetics of adriamycin and adriamycinol—Implications for the design of invitro experiments and treatment protocols," Cancer Res. **43**, 3417–3421 (1983).
[28]K. M. Laginha, S. Verwoert, G. J. R. Charrois, and T. M. Allen, "Determination of doxorubicin levels in whole tumor and tumor nuclei in murine breast cancer tumors," Clin. Cancer Res. **11**, 6944–6949 (2005).
[29]C. M. Ma, D. Cvetkovic, X. Chen, and L. Chen, "Non-thermal pulsed focused ultrasound for cancer therapy," Med. Phys. **38**, 3824–3824 (2011).

MR-guided pulsed high intensity focused ultrasound enhancement of docetaxel combined with radiotherapy for prostate cancer treatment

2012 Phys. Med. Biol. 57 535

(http://iopscience.iop.org/0031-9155/57/2/535)

IOP Publishing Physics in Medicine and Biology
Phys. Med. Biol. **57** (2012) 535–545 doi:10.1088/0031-9155/57/2/535

MR-guided pulsed high intensity focused ultrasound enhancement of docetaxel combined with radiotherapy for prostate cancer treatment

Zhaomei Mu[1], C-M Ma[1], Xiaoming Chen[1], Dusica Cvetkovic[1], Alan Pollack[2] and Lili Chen[1,3]

[1] Department of Radiation Oncology, Fox Chase Cancer Center, Philadelphia, PA, USA
[2] Department of Radiation Oncology, Sylvester Comprehensive Cancer Center, Miller School of Medicine, University of Miami, Miami, FL, USA

E-mail: lili.Chen@fccc.edu

Received 25 August 2011, in final form 26 August 2011
Published 4 January 2012
Online at stacks.iop.org/PMB/57/535

Abstract
The purpose of this study is to evaluate the efficacy of the enhancement of docetaxel by pulsed focused ultrasound (pFUS) in combination with radiotherapy (RT) for treatment of prostate cancer *in vivo*. LNCaP cells were grown in the prostates of male nude mice. When the tumors reached a designated volume by MRI, tumor bearing mice were randomly divided into seven groups ($n = 5$): (1) pFUS alone; (2) RT alone; (3) docetaxel alone; (4) docetaxel + pFUS; (5) docetaxel + RT; (6) docetaxel + pFUS + RT, and (7) control. MR-guided pFUS treatment was performed using a focused ultrasound treatment system (InSightec ExAblate 2000) with a 1.5T GE MR scanner. Animals were treated once with pFUS, docetaxel, RT or their combinations. Docetaxel was given by i.v. injection at 5 mg kg^{-1} before pFUS. RT was given 2 Gy after pFUS. Animals were euthanized 4 weeks after treatment. Tumor volumes were measured on MRI at 1 and 4 weeks post-treatment. Results showed that triple combination therapies of docetaxel, pFUS and RT provided the most significant tumor growth inhibition among all groups, which may have potential for the treatment of prostate cancer due to an improved therapeutic ratio.

(Some figures may appear in colour only in the online journal)

1. Introduction

Focused ultrasound (FUS) has clinically emerged as a noninvasive therapy technique for localized prostate cancer and other solid malignancies (Kennedy 2005). For clinical treatment,

[3] Author to whom any correspondence should be addressed

0031-9155/12/020535+11$33.00 Printed in the UK & the USA

FUS is predominantly being used for thermal ablation in targeted tissues by continuous deposition of focused acoustic energy. Pulsed FUS (pFUS) uses nonthermal effects at low duty cycles that alter the tissue properties. Recent studies have suggested that pFUS exposure may alter vascular or cell membrane permeability to enhance drug delivery in tumors in animal models (Bednarski *et al* 1997, Nelson *et al* 2002, Dittmar *et al* 2005, Yuh *et al* 2005, Frenkel *et al* 2006, Hancock *et al* 2009, Chen *et al* 2010). Enhancement of drug delivery to the tumor target by pFUS exposures and its effect on tumor growth inhibition *in vivo* has been reported by other investigators (Dittmar *et al* 2005, Dromi *et al* 2007, Poff *et al* 2008).

Radiation therapy (RT) is one of the primary treatments for prostate cancer. Although there has been a reduction in failure rates with increased RT dose using sophisticated planning and delivery techniques, local persistence of disease remains in many cases (Hanks *et al* 1998, Pollack *et al* 2002, Jacob *et al* 2004). Androgen deprivation (AD) is one of the most common additional treatments for advanced prostate cancer. Chemotherapy has been shown to prolong median survival for hormone refractory disease (Tannock *et al* 2004, Petrylak *et al* 2004). Docetaxel has become the standard first-line chemotherapy for the treatment of advanced hormone refractory prostate cancer (Armstrong and George 2010).

In our laboratory, we have developed techniques for prostate tumor implantation orthotopically. In a previous study, we developed MR-guided focused ultrasound (MRgFUS) treatment techniques for a small animal model (nude mouse) using a clinical patient treatment device (InSightec ExAblate 2000) together with a 1.5 T MR scanner (Signa Excite HD, GE Healthcare, Milwaukee, WI, USA) for MR guidance during treatment. We performed *in vivo* experiments to investigate the use of MRgFUS for the enhancement of chemotherapy in prostate tumors grown in nude mice using [^{3}H]-docetaxel. Our experimental data showed that the [^{3}H]-docetaxel concentration in tumors treated with MRgFUS was significantly increased compared with those without the MRgFUS treatment (Chen *et al* 2010). The purpose of this study is to investigate whether the enhancement of the docetaxel uptake using MR-guided pFUS combined with RT will improve the tumor response *in vivo*.

2. Methods and materials

2.1. Cell culture and tumor model

Human prostate cancer LNCaP cells were obtained from the American Type Culture Collection and cultured in Dulbecco's modified Eagle's medium (DMEM)-F12 medium, containing 10% fetal bovine serum (FBS), 1% L-glutamine and 1% penicillin-streptomycin as described previously (Mu *et al* 2008). Male athymic Balb/c nude mice (6 weeks old) were purchased from Harlan (Indianapolis, IN). All animal studies were carried out in compliance with approval of both the institutional animal care and use committee (IACUC) and the institutional radiation safety committee. Aseptic techniques were used for injection and implantation of LNCaP cells in the prostates of nude mice as described previously (Mu *et al* 2008, Stoyanova *et al* 2007, Chen *et al* 2010). Nude mice were anesthetized using methoxyflurane. A lower midline incision was made approximately 1.5 cm above the presumed location of the bladder. The seminal vesicles were gently brought out through the incision and LNCaP cells (1×10^6) in 25 μl of PBS (phosphate buffered saline) were injected into the dorsal prostate lobes using a 30-gauge 1-inch needle. The incision was sealed by suturing the muscle layer (suture size-4.0 silk) and 2–3 wound clips for the skin layer.

2.2. MR imaging

2.2.1. Tumor volume measurement. Beginning at 3 weeks after the tumor implantation the tumor volume was monitored weekly by MRI in a vertical wide-bore magnet equipped with a Bruker DRX 300 console at a field strength of 7 tesla. The standard MR imaging protocol was provided by the small animal imaging facility at Fox Chase Cancer Center (FCCC), as described previously (Stoyanova *et al* 2007). Briefly, the tumor volumes were determined by outlining tumors using the Paravision software supplied with the spectrometer, and then summing the volumes from all the sections. The images were made with a two-dimensional multislice spin echo pulse sequence. Repetition times were in the range of 400–600 ms, the echo time was 13.2 ms, the slice thickness was 0.75 mm and the in-plane resolution was 0.1 mm. Signal averaging over two acquisitions brought the scan time to less than 4 min. This protocol allowed us to visualize tumors with volumes as small as 5 mm^3. Animal preparation and scout image acquisition brought the total MR imaging time to approximately 10 min per animal. Prior to imaging, the mouse received an injection of 0.2 ml of the commercial contrast agent Magnevist (Berlex Industries-Montville, NJ) diluted 10:1 with a physiological concentration of saline. During imaging the mouse was anesthetized with a mixture of 1% isofluorane in oxygen. When the tumor volume reached a designated size (see below) treatments were initiated.

2.2.2. MRI for FUS. The 'optimal' MR imaging protocol for MRgFUS treatment with the 1.5 T scanner used in this study was based on our previous study (Chen *et al* 2010). The protocol provides a high-quality image to identify the prostate tumor in a nude mouse within approximately 1 h anesthesia time for the entire treatment procedure. The scans were first performed for localization (three-dimensional) using a fast spin echo (FSE) image sequence at low image quality with a 0.13 min scan time and then for the coronal image sequence with a 7 min scan time to achieve high-quality imaging for tumor target identification. The MR parameters were T2-weighted coronal FSE sequence; TR/TE = 2150/102 ms; bandwidth = 10.4 kHz; FOV = 9.0 × 9.0 cm; matrix: 384 × 384; NEX = 4; slice thickness = 2.0 mm/0.0 sp; frequency direction: SI and the spatial resolution: 0.23 mm. Based on the coronal image, an axial FSE sequence was performed with a 4.25 min scan time. Figure 1(A) shows an example of the high-quality images used for tumor delineation and treatment planning in real time for this study.

2.3. Experimental setup

An ExAblate 2000 FUS system (InSightec-Tx-Sonics, Haifa, Israel and Dallas, TX) together with a 1.5 T GE MR scanner was used for the pFUS treatment (figure 1(B)). The system was installed in the Department of Radiation Oncology at FCCC in 2006. This treatment system was approved by the FDA for treating uterine fibroids clinically. In our department it is being used for treatment of painful bone metastases (Chen *et al* 2009), for preclinical investigations of prostate and breast cancer ablation under the local Institutional Review Board (IRB) approval (Ma *et al* 2009).

Quality control (QC) for the FUS treatment unit was performed according to the procedures provided by the vendor to check the transducer output, the focal spot and the electronic motion system before animal treatments as described previously (Chen *et al* 2010). Mice were anesthetized by intraperitoneal injection of a mixture of ketamine (60 mg kg^{-1}) and ace-promazine (2.5 mg kg^{-1}). Figure 1(B) shows the animal setup for pFUS treatments. A gel pad was placed on the treatment table in line with the transducer. Degassed water was

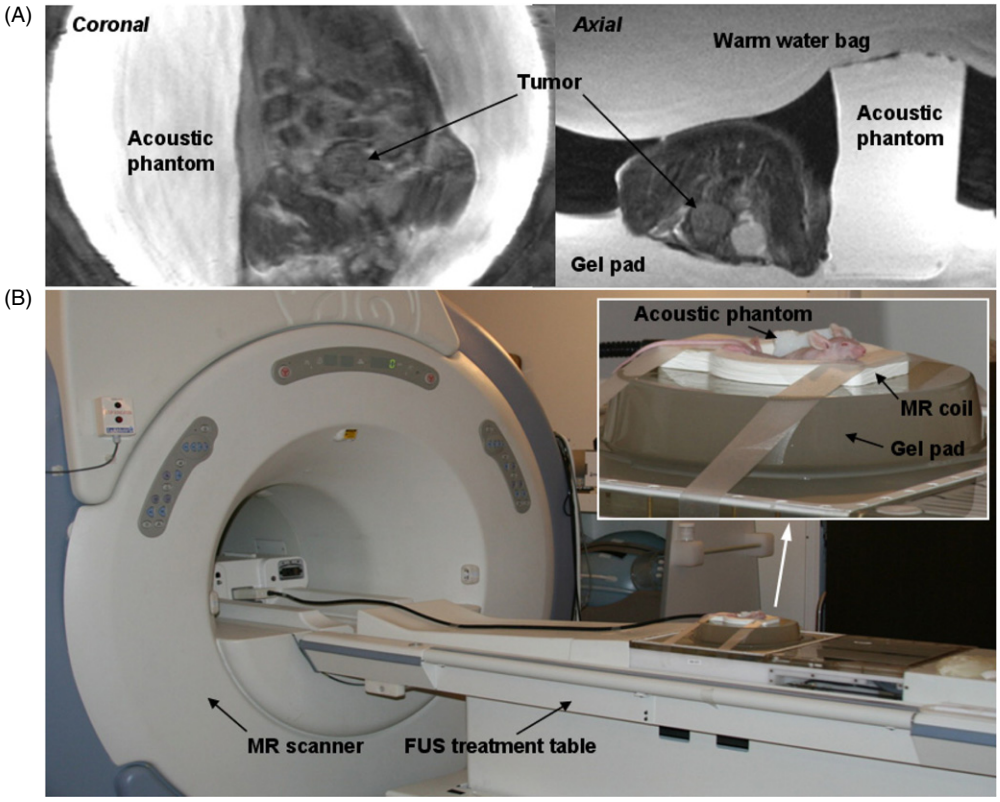

Figure 1. (A) MR images showing prostate tumors in a coronal view and an axial view obtained on a 1.5 T MR scanner. (B) The FUS treatment table with a 1.5 T MR scanner and the animal setup for the pFUS treatment.

used for the interface between the treatment table and the gel pad for the acoustic coupling. Mice were carefully placed in the hole (approximately 5 cm $\times$ 5 cm $\times$ 1 cm) of the gel pad, which was filled with degassed water. A 3 inch surface coil was placed around the animal to receive the MR signals. A small (4 cm $\times$ 2 cm $\times$ 2 cm) acoustic phantom provided by the vendor was placed beside the mouse for verification of the location of the focal spot prior to animal sonication (figure 1). The acoustic phantom was manufactured by ATS Labs Inc. (Bridgeport, CT) with acoustic properties similar to those of human soft tissue (the attenuation coefficient = 0.503 dB cm^{-1} MHz^{-1}; speed of sound= 1538 MPS; estimated specific heat= 2.684 cal/g). The phantom was not used for the validation of thermometry as the thermal conductivity of the phantom was not available. A surgical glove filled with warm water was placed on top of the mouse to protect the animal from hypothermia.

2.4. Pulsed focused ultrasound treatment

Pulsed-FUS treatment was performed using a method described in detail in a previous publication (Chen *et al* 2010). Briefly, both coronal and axial MR images were loaded on the focused ultrasound treatment workstation. The tumor was contoured, the skin surface was delineated and a treatment plan was generated. Prior to focused ultrasound treatment, the

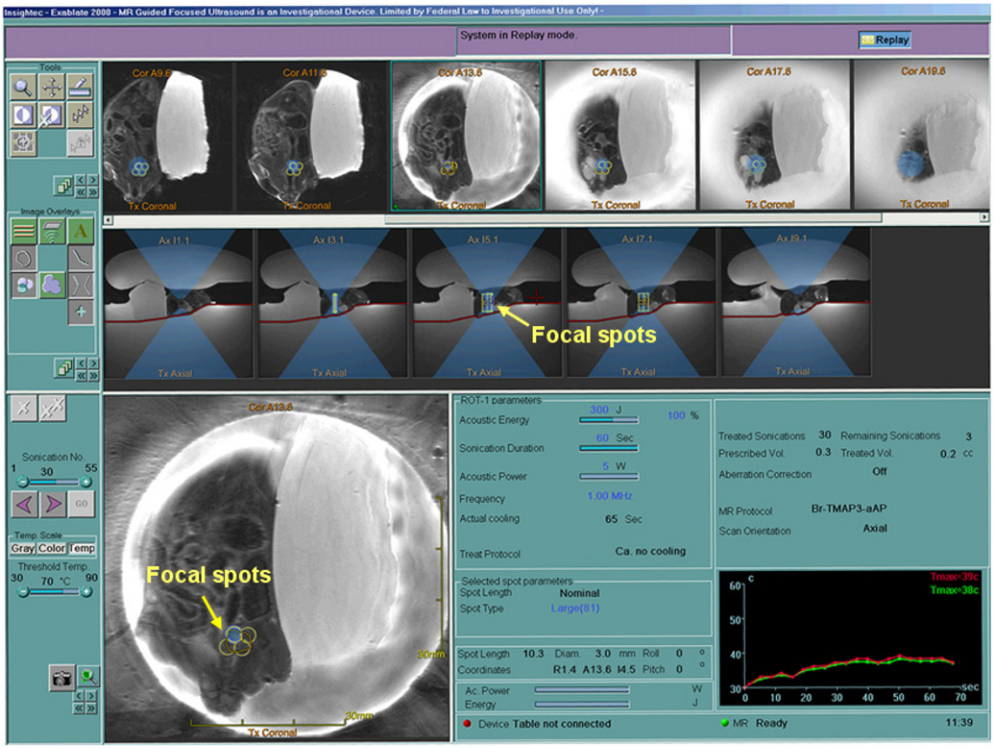

Figure 2. A FUS treatment plan with multiple focal spots (arrows) covering the tumor target on both coronal and axial images. The real-time temperature was monitored by MR thermometry.

effective focal spot was verified using the small acoustic phantom beside the animal using MR thermometry. Animals were treated using the following parameters: 1 MHz; 5 W acoustic power for 60 s with 50% duty cycle (0.1 s power on and 0.1 s power off) per sonication, depending on the experimental design (see below). The time-averaged acoustic focal intensity was approximately 220 W cm^{-2} estimated using the acoustic power and the beam cross-sectional area. The treatment parameters were derived from our acoustic phantom studies as described by Chen *et al* (2010). The whole tumor volumes were covered with multiple focal spots depending on the tumor sizes. Figure 2 shows real-time treatment planning for the pFUS treatment. The tumor target was covered by multiple focal spots on both the coronal and axial MR images. The temperature was monitored in real-time (~3 s delay) by MR thermometry.

2.5. Study design

Study 1: This is a pilot study aimed to determine a reasonable docetaxel dose and the FUS treatment scheme. When the tumor volume reached 45 ± 8.5 mm^3 on MRI, mice were randomly assigned to four groups ($n = 5$): (1) pFUS alone; (2) pFUS + docetaxel; (3) docetaxel alone, and (4) control. For groups 1 and 2, each mouse was treated with pFUS under general anesthesia for two fractions (one treatment per week for two consecutive weeks). For groups 2 and 3, each animal received docetaxel (Taxotere; sanofi-aventis U.S. LLC, Bridgewater, NJ) by tail vein injection at 10 mg kg^{-1} for two fractions (one injection per week for two consecutive weeks). For group 2 the docetaxel was injected immediately after the pFUS

treatment. For the control group, a sham FUS treatment was given. Animals were allowed to survive for 4 weeks. The tumor volumes were measured by MR imaging at 1 and 4 weeks after the treatment.

Study 2: Based on the results from study 1, both the docetaxel dose and the pFUS treatment scheme were adjusted to reduce the systemic toxicities. When the tumor volume reached 36 $\pm$ 5.9 mm^3 on MRI, mice were randomly divided into seven groups ($n = 5$): (1) pFUS alone; (2) RT alone; (3) docetaxel only; (4) docetaxel + pFUS; (5) docetaxel + RT; (6) docetaxel + pFUS + RT, and (7) control. Animals receiving the pFUS treatment were only treated once. Animals receiving the docetaxel treatment were also treated once and the dose was reduced to 5 mg kg^{-1}. The docetaxel injection was performed before the pFUS and RT treatment was performed immediately after the pFUS. For the RT treatment, animals were restrained under general anesthesia in the supine position with tape in a jig and irradiated on a Cesium 137 irradiator (model 81-14; J.L. Shepherd and Associates, San Fernando, CA). A collimator was used to treat the prostate while protecting the lung, abdomen and legs (Stoyanova *et al* 2007). Animals were allowed to survive for 4 weeks. Tumor volumes were measured by MRI at 1 and 4 weeks after the treatment.

2.6. Data analysis and statistics

The relative tumor volume (TV) for each animal was calculated as a ratio of the tumor volume at 1 and 4 weeks after treatment to the tumor volume on the treatment day. Statistical analysis was done using the Statistical Package for the Social Sciences (SPSS). The one-way ANOVA least significance difference test (LSD) was used to determine the significance among experimental groups, and $P < 0.05$ was considered significant.

3. Results

Our first pilot study (study 1) was designed to find a reasonable docetaxel dose and the pFUS treatment scheme for our investigation. Figure 3 shows the relative TV change at 1 week and 4 weeks after the pFUS and docetaxel treatment. Tumor growth delay was observed for the group receiving pFUS alone at 1 week and 4 weeks after the treatment; the average tumor volume was 28.3% and 39% smaller compared to that of the control group, respectively. The tumor growth delay was more significant for the group receiving docetaxel only; the average tumor volume at 1 week after treatment was smaller than that prior to the treatment ($P = 0.0013$) and it only increased slightly 4 weeks post-treatment ($P = 0.0028$). It should be mentioned that the tumor volume measured by MRI within a short period of time (e.g. 1 week) after the treatment might not accurately reflect the actual number of surviving tumor cells because both chemo/radiotherapy would thin out tumor cells randomly in the tumor volume rather than changing the tumor bulk volume/shape. The tumor volume at 4 weeks after treatment would be a better indicator of the total viable tumor cells when it grew significantly greater than that prior to the treatment. The combination of pFUS and docetaxel showed excellent tumor control; the average tumor volume was smaller than that prior to the treatment both 1 week and 4 weeks after treatment. However, their overwhelming cell killing power, especially that by docetaxel, also drowned out the potential synergistic effect of pFUS and docetaxel.

Although docetaxel alone at a dose of 10 mg kg^{-1} for two consecutive weeks resulted in a significant delay in tumor growth, the associated toxicities were also severe to the small animals (the average body weight of the nude mice was 25 g). Results from study 1 showed that the animals did not tolerate the 2-week treatment very well; the docetaxel-treated mice suffered severe weight loss (>10% body weight) and an approximately 30% mortality. The

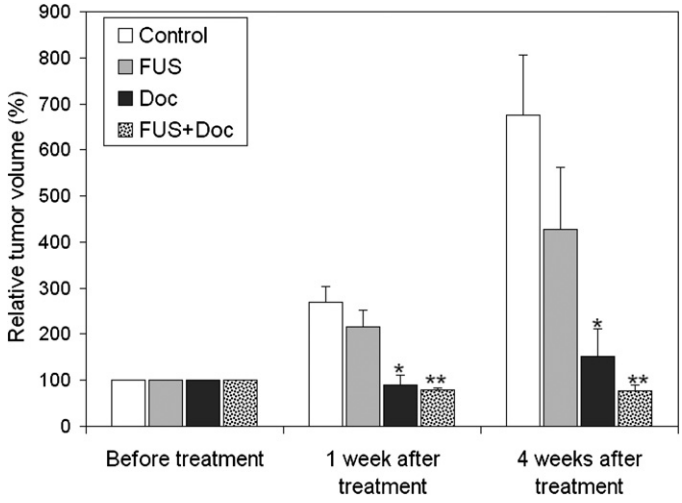

Figure 3. Relative tumor volume at 1 and 4 weeks after the 2-week treatment with docetaxel (10 mg kg^{-1}, 2 fractions), pFUS (2 fractions) or the combination of the two, relative to the average tumor volume prior to the treatment. Error bars are standard deviation of the mean. $^{*}P < 0.05$ and $^{**}P < 0.05$ compared with the control and FUS groups (one-way ANOVA, LSD test).

pFUS-treated mice also lost weight (about 10%) during the 2-week treatment (recovered 4 weeks after treatment), which was probably due to the effect of the general anesthesia since the animals could not have normal intake for the entire treatment day. There was a concern that severe treatment toxicities might adversely affect the experimental accuracy on the tumor growth. The second study was therefore designed to reduce the treatment toxicities and mortality.

In study 2, the docetaxel dose was lowered to 5 mg kg^{-1} (mouse body weight) with only one injection to reduce the side effects of chemotherapy. The pFUS treatment was given once only to minimize the possible effect due to general anesthesia. The docetaxel injection was given immediately before the FUS/RT treatment to enhance drug penetration/absorption, assuming that the docetaxel concentration was still at or near its peak value when pFUS altered the permissibility of the vessel wall and the cell membrane. Figure 4 shows the relative tumor volume based on the experimental results from the second study. The relative tumor volume and the associated uncertainty are given in table 1. Animals treated with pFUS alone showed a small (about 4%) reduction in the average tumor volume at 4 weeks after the treatment compared to the control group, but it was not statistically significant ($P = 0.45$). The tumor growth delay was more than 37% for the RT alone group 4 weeks after a 2 Gy irradiation, which is a typical daily dose for standard-fractionation radiation therapy. The tumoricidal effect of docetaxel at 5 mg kg^{-1} was still significant; the average tumor volume 4 weeks post-treatment was about 60% smaller than that of the control group. The level of inhibition achieved with dual combination therapy of docetaxel + FUS or of docetaxel + RT was not statistically different from that with docetaxel alone ($P = 0.39$ and 0.37 respectively). The tumor volume for the group receiving triple combination therapy of docetaxel + pFUS + RT appeared to be the lowest compared to all treatment groups (table 1). Further experiments are needed to quantify the therapeutic ratio of dual or triple combination therapies of docetaxel with FUS and/or RT in terms of the dose level and fractionation scheme.

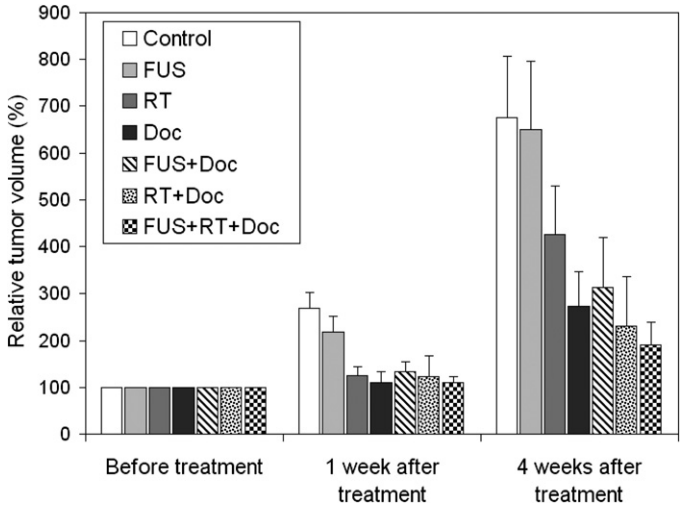

Figure 4. Relative tumor volume at 1 and 4 weeks after the single-fraction treatment of docetaxel (5 mg kg^{-1}), pFUS, RT and dual- or triple combination therapies of the three modalities, relative to the average tumor volume prior to the treatment. The error bars are standard deviation of the mean.

Table 1. Relative tumor volumes at 1 and 4 weeks after treatments.

	Relative tumor volume[a] (Mean ± SEM[b])	
Group	1 week	4 weeks
Control	2.69 ± 0.34	6.76 ± 1.30
FUS	2.19 ± 0.33	6.50 ± 1.46
RT	1.25 ± 0.18	4.26 ± 1.04
Doc	1.11 ± 0.23	2.73 ± 0.73
FUS + Doc	1.34 ± 0.20	3.13 ± 1.06
RT + Doc	1.24 ± 0.44	2.31 ± 1.06
FUS + RT + Doc	1.10 ± 0.13	1.91 ± 0.47

[a] Ratio of tumor volume after the treatment to that before the treatment.
[b] SEM: standard deviation of the mean.

4. Discussion and summary

In our previous study, a technique was established that is capable of performing pFUS on nude mice with implanted prostate tumors using a clinical treatment equipment. The results from our *in vivo* studies demonstrated the pFUS enhancement of the docetaxel delivery. The purpose of this study is to investigate if the increased uptake of docetaxel would result in tumor growth inhibition *in vivo*.

Although some effects of pFUS on tumor growth inhibition were observed using the described treatment parameters compared to the control group, our results did not yield statistically significant differences between them with the current small sample numbers ($n = 5$). This was consistent with the findings of other solid tumor model studies (Dittmar *et al* 2005, Dromi *et al* 2007, Poff *et al* 2008, Frenkel *et al* 2006). However, one study showed

that mechanical FUS with different treatment parameters might induce antitumor immunity and therefore reduce tumor growth in a murine tumor model (Hu *et al* 2007).

The pFUS exposure with an acoustic power of 5 W used in this study generated a temperature elevation less than 5 °C in targeted tumor tissues (to ensure a temperature of <42 °C for potential future human applications) (Chen *et al* 2010). The MR proton resonance frequency shift sequence (machine built-in software) was used for monitoring the temperature changes during the pFUS treatment (figure 2). Our prior results have shown that the ^{3}H-docetaxel delivery in implanted tumors can be enhanced by pFUS using the same treatment parameters.

Increasing experimental and theoretical results have indicated that pulsed FUS can enhance the permeability of target tissues or change the structure of extracellular matrix to improve drug or gene delivery (i.e. Frenkel and Li 2006). A recent study showed that pFUS generated acoustic radiation forces produced in the targeted tissue may have a role in enhancing delivery (Hancock *et al* 2009). The mechanisms for producing the observed enhancement are not well understood. It is thought mainly due to the nonthermal effects of ultrasound—mechanical streaming and cavitation although larger increases in temperature could occur within microenvironments of the cell as a result of cavitation. The increased extravasation of the blood was observed in our previous study using the same ultrasonic parameters as for this study. Our results suggested that the increase drug delivery in tumor was a result of the increased blood vessel permeability. The possible mechanisms have been discussed in our previous published paper (Chen *et al* 2010). However, the precise mechanism is little known and needs to be further investigated. Extensive histological studies are being conducted on prostate tumors treated with pFUS to answer these questions.

Radiation is one of the most effective treatment modalities for prostate cancer. Docetaxel is one of the few effective drugs for the treatment of advanced hormone refractory prostate cancer and/or metastatic disease clinically. Docetaxel inhibits microtubule formation and downregulates antiapoptotic protein Bcl-2 expression (Engels *et al* 2005). Furthermore, the combination of docetaxel and bortezomib as a chemotherapeutic drug sensitizes Bcl-2 overexpressing human prostate cancer cells to radiation effects by modulating the expression of key members of the Bcl-2 family (Cao *et al* 2008). In the present study, we chose to test the efficacy of pFUS, docetaxel and RT alone and dual- or triple-combination therapies using an orthotopic prostate cancer model. Our results showed that both docetaxel and RT alone caused a significant increase in tumor growth inhibition compared with the control group. The strong effect of docetaxel on tumor growth was observed with both double injections of 10 mg kg^{-1} and a single injection of 5 mg kg^{-1}. However, the radiation-sensitizing effect of docetaxel was not evident when docetaxel and RT were given together (Cao *et al* 2008). When pFUS was given prior to the injection of 10 mg kg^{-1} docetaxel, there was a further delay in tumor growth compared to treating with pFUS or docetaxel alone (figure 3). However, when docetaxel was injected at a lower dose of 5 mg kg^{-1} prior to the pFUS treatment, there was no further tumor growth inhibition for the limited number of animals investigated (figure 4). The lowest level of tumor growth was seen when all three treatments, pFUS, docetaxel and RT were given together. Our results suggested that the *in situ* dose of docetaxel might be very uncertain between individual mice, which may have an impact on the determination of tumor growth inhibition especially when combined with other therapies. The variation of the blood flow among individual animals may have contributed to the uncertainty in the measured drug-dose response. The standard deviation of the tumor volume was also higher than expected, which may also have an impact on the drug-dose response. A larger sample may help reduce the overall experimental uncertainty. Because docetaxel alone at both dose levels of 5 mg kg^{-1} and 10 mg kg^{-1} already resulted in significant tumor cell killing, additional antitumor effects from

pFUS or RT may become less pronounced, at least with our current number of animals used. A similar study showed pFUS enhanced tumor growth inhibition with a chemotherapeutic drug, botezomib, at a low dose level; drug alone had no effect on the tumor growth (Poff *et al* 2008).

In summary, we have performed experiments to investigate the effectiveness of the increased uptake of docetaxel by pFUS in combination with RT in prostate tumor control *in vivo*. Although previous studies have demonstrated the antitumor efficacy of pFUS in combination with a variety of therapeutic agents at different settings and using different tumor models by other investigators, the results from this study did not show significant synergistic effects between docetaxel, pFUS and RT. However, this study was performed with a small sample and only a single animal tumor model. Future studies are being designed to continue investigating the drug enhancement effect of pFUS by focusing on optimal pFUS treatment parameters and chemo/gene dose levels and fractionation schemes.

Acknowledgments

We would like to thank Dr Harvey Hensley for his technical assistance with MRI using the 7T MR scanner, the small animal imaging facility and the animal care facility at Fox Chase Cancer Center. We would also like to thank InSightec, especially Dr Arik Hananel, Ms Osnat Dogadkin, Mr Amit Sokolov, Javier Grinfeld MSc and Dr Jessica Foley for their excellent technical support. This study was supported by the Focused Ultrasound Surgery Foundation and DOD (PC073127).

References

Armstrong A J and George D J 2010 Optimizing the use of docetaxel in men with castration-resistant metastatic prostate cancer *Prostate Cancer Prostatic Dis.* **13** 108–16

Bednarski M D, Lee J W, Callstrom M R and Li K C 1997 *In vivo* target-specific delivery of macromolecular agents with MR-guided focused ultrasound *Radiology* **204** 263–8

Cao W, Shiverick K T, Namiki K, Sakai Y, Porvasnik S, Urbanek C and Rosser C J 2008 Docetaxel and bortezomib downregulate Bcl-2 and sensitize PC-3-Bcl-2 expressing prostate cancer cells to irradiation *World J. Urol.* **26** 509–16

Chen L, Ma C-M, Richardson T, Freedman G and Konski A 2009 Treatment of bone metastasis using MR guided focused ultrasound *Med. Phys.* **36** 2486 (Abstract)

Chen L, Mu Z, Hachem P, Ma C-M, Wallentine A and Pollack A 2010 MR-guided focused ultrasound: enhancement of intratumoral uptake [3H]-docetaxel *in vivo Phys. Med. Biol.* **55** 7399–410

Dittmar K M, Xie J, Hunter F, Trimble C, Bur M, Frenkel V and Li K C 2005 Pulsed high-intensity focused ultrasound enhances systemic administration of naked DNA in squamous cell carcinoma model: initial experience *Radiology* **235** 541–6

Dromi S *et al* 2007 Pulsed-high intensity focused ultrasound and low temperature-sensitive liposomes for enhanced targeted drug delivery and antitumor effect *Clin. Cancer Res.* **13** 2722–7

Engels F K, Sparreboom A, Mathot R A and Verweij J 2005 Potential for improvement of docetaxel-based chemotherapy: a pharmacological review *Br. J. Cancer* **93** 173–7

Frenkel V, Etherington A, Greene M, Quijano J, Xie J, Hunter F, Dromi S and Li K C 2006a Delivery of liposomal doxorubicin (Doxil) in a breast cancer tumor model: investigation of potential enhancement by pulsed-high intensity focused ultrasound exposure *Acad. Radiol.* **13** 469–79

Frenkel V and Li K C 2006b Potential role of pulsed-high intensity focused ultrasound in gene therapy *Future Oncol.* **2** 111–9

Hancock H A, Smith L H, Cuesta J, Durrani A K, Angstadt M, Palmeri M L, Kimmel E and Frenkel V 2009 Investigations into pulsed high-intensity focused ultrasound-enhanced delivery: preliminary evidence for a novel mechanism *Ultrasound Med. Biol.* **35** 1722–36

Hanks G E, Hanlon A L, Schultheiss T E, Pinover W H, Movsas B, Epstein B E and Hunt M A 1998 Dose escalation with 3D conformal treatment: five year outcomes, treatment optimization, and future directions *Int. J. Radiat. Oncol. Biol. Phys.* **41** 501–10

Hu Z *et al* 2007 Investigation of HIFU-induced anti-tumor immunity in a murine tumor model *J. Transl. Med.* **5** 34

Jacob R, Hanlon A L, Horwitz E M, Movsas B, Uzzo R G and Pollack A 2004 The relationship of increasing radiotherapy dose to reduced distant metastases and mortality in men with prostate cancer *Cancer* **100** 538–43

Kennedy J E 2005 High-intensity focused ultrasound in the treatment of solid tumours *Nat. Rev. Cancer* **5** 321–7

Ma C-M CL *et al* 2009 MR guided focused ultrasound for high risk and recurrent breast cancer *WC, IFMBE Proc. 25/VI* ed O Dössel and W C Schlegel (Heidelberg: Springer) pp 140–3

Mu Z, Hachem P, Hensley H, Stoyanova R, Kwon H K, Hanlon A L, Agrawal S and Pollack A 2008 Antisense MDM2 enhances the response of androgen insensitive human prostate cancer cells to androgen deprivation *in vitro* and *in vivo Prostate* **68** 599–609

Nelson J L *et al* 2002 Ultrasonically activated chemotherapeutic drug delivery in a rat model *Cancer Res.* **62** 7280–3

Petrylak D P *et al* 2004 Docetaxel and estramustine compared with mitoxantrone and prednisone for advanced refractory prostate cancer *N. Engl. J. Med.* **351** 1513–20

Poff J A, Allen C T, Traughber B, Colunga J, Xie Z, Chen B J, Wood C, Waes V, Li K C and Frenkel V 2008 Pulsed high-intensity focused ultrasound enhances apoptosis and growth inhibition of squamous cell carcinoma xenografts with proteasome inhibitor bortezomib *Radiology* **248** 485–91

Pollack A, Zagars G K, Antolak J A, Kuban D A and Rosen II 2002 Prostate biopsy status and PSA nadir level as early surrogates for treatment failure: analysis of a prostate cancer randomized radiation dose escalation trial *Int. J. Radiat. Oncol. Biol. Phys.* **54** 677–85

Stoyanova R, Hachem P, Hensley H, Khor L Y, Mu Z, Hammond M E, Agrawal S and Pollack A 2007 Antisense-MDM2 sensitizes LNCaP prostate cancer cells to androgen deprivation, radiation, and the combination *in vivo Int. J. Radiat. Oncol. Biol. Phys.* **68** 1151–60

Tannock I F *et al* 2004 Docetaxel plus prednisone or mitoxantrone plus prednisone for advanced prostate cancer *N. Engl. J. Med.* **351** 1502–12

Yuh E L, Shulman S G, Mehta S A, Xie J, Chen L, Frenkel V, Bednarski M D and Li K C 2005 Delivery of systemic chemotherapeutic agent to tumors by using focused ultrasound: study in a murine model *Radiology* **234** 431–7

distribution of viable tissue. **Results:** Averaging effects associated with PET imaging altered the true 3D spatial pattern of FDG intratumoral uptake. ROC analysis indicated good sensitivity of FDG PET image-segmentation for the detection of the viable tissue (AUC = 0.74). However, the specificity was low, as indicated by the low threshold value at which the maximum overlap occurred (22% of maximum uptake).**Conclusion:** A novel method of histopathological validation of PET imaging for image-guidance in radiotherapy was developed. Using this method, it was demonstrated that for the tumors with high viable tissue content, FDG-thresholding can be used for viable tissue detection.

TH-E-BRA-03

Clinical Experience at Fox Chase Cancer Center for Treatment of Bone Metastases Using ExAblate 2000 with MR Guidance

L Chen*, C Ma, T Richardson, G Freedman, A Konski, X Chen, J Fan, R Price, J Meyer, Fox Chase Cancer Center, Philadelphia, PA

Purpose: To evaluate the safety and efficacy of MR guided focused ultrasound (MRgFUS) treatment for bone metastases. **Methods:** Six patients with scapula (2), humeral head, sacrum, ilium and pubic ramus bone metastases were treated using ExAblate 2000 under MR guidance. In addition to the monthly and annual quality assurance (QA), pre-treatment machine calibration was performed before each treatment including the functionality of the treatment software and the mechanical motion control systems. The effective ultrasound focal spot was verified with an acoustic phantom using MR thermometry. The patient was positioned on a gel pad. The interface between the treatment table, the gel pad and the patient was immersed in degassed water for acoustic coupling. Caution was taken to remove all gas bubbles between the interfaces. Treatment was performed under conscious sedation. Six to eighteen sonications were delivered for each patient treatment depending on each lesion's size. Patients were treated with a frequency of 1 MHz; 32 ± 4.0 to 96 ±11W acoustic power and 628 ± 78 to1859 ± 338J energy for 20-30s for each sonication. MR phase images were used to monitor the temperature changes in real-time. Based on the temperature feedback, the acoustic power was adjusted to reach designed temperatures (=60 °C) for individual sonications. Pain was assessed using the visual analog scale (VAS). **Results:** All patients tolerated the MRgFUS treatment well. No skin toxicity or other complications were observed. The VAS pain rating was significantly reduced for all 6 patients from 8.2 ± 0.8 before treatment to 4.7 ± 3, 2.7 ± 1.5 and 1.8 ± 1.1 at one day, one month and three months respectively. **Conclusions:** A comprehensive QA program has been developed for the MRgFUS system. Our data suggest that MRgFUS is a safe, effective and noninvasive treatment modality for palliation of bone metastases.

TH-E-BRA-04

Feasibility of Mapping Transient Tumor Hypoxia Using in Situ Activation PET Imaging: A Simulation Study

E Dalah[1]*, c yang[2], I Moraru[3], E Paulson[4], Q Zhang[5], Y Hu[6], X Li[7], (1) Medical College of Wisconsin, Milwaukee, WI, (2) , , , (3) Medical College of Wisconsin, Milwaukee, WI, (4) Medical College of Wisconsin, Milwaukee, WI, (5) 2Wu Xi Yi Ren Tumor Hospital, Wu Xi, Jiang Su, (6) Cancer Institute, CAMS, Beijing, , (7) Medical College of Wisconsin, Milwaukee, WI

Purpose: Detecting transient tumor hypoxia in real-time is desirable and has been challenging in radiation therapy. Here, we explore the feasibility of mapping tumor transient hypoxia in real-time using in situ activation by high-energy photons. **Methods:** The simulation used spatial uptake of a hypoxia tracer (e.g. 64Cu-ATSM) in PET or autoradiograph as a surrogate for micro-vessel density, which was then used to generate a steady state oxygen tension (pO2) map using a reaction diffusion model. The 15O in situ activation map by high-energy photons was generated using Ten Haken model based on the steady state pO2 map with the addition of element composition. The activation map includes both mobile and immobile 15O. The mobile 15O component was isolated by subtracting the fast decay portion from the overall decay curve. The simulation process was coded in Matlab using photon energies of 20 - 50MeV. **Results:** The diffusion model shows heterogeneous distribution of pO2 ranges from 28 - 1.9 mmHg for a pancreas tumor model, depending on simulation baseline values, tumor vasculature structure and architecture. The threshold of 63% of the mean image intensity on the in situ activation PET image was found to reasonably agree with original hypoxia map using 5 mmHg as a cutoff value. The simulated transient hypoxic fraction was comparable with measurements reported using 64Cu-ATSM autoradiography, e.g., measurement of 0.166 ± 0.067 versus simulation of 0.157. **Conclusions:** It is feasible to detect transient tumor hypoxia with oxygen in situ activation using high-energy photons. This opens door for tracking tumor transient hypoxia in real-time during the delivery of radiation therapy. Immediate future work includes quantifying the in situ activation PET (e.g., 15O activity in terms of pO2 in mmHg), and in-vivo measurement of the in situ activation.

TH-E-BRA-05

Improving the Contrast of Proton and Carbon Radiography by Using CT Prior Knowledge

M Spadea[1], A Fassi[2], N Depauw[3]*, M Riboldi [2], G Baroni[2], J Seco[3], (1) Magna Graecia University, Italy (2) Politecnico di Milano University, Italy, (3) Mass General Hospital; Harvard Medical, Boston , MA (4) Center for Medical Radiation Physics (CMRP), University of Wollongong (UoW), Wollongong, NSW, Australia

Purpose: To enhance the quality of proton/carbon radiography for real time tumor tracking using CT prior knowledge. **Methods:** A method for contrast enhancement was applied to particle radiographies (230 MeV proton, 330 MeV proton, 500MeV/n Carbon) virtually generated by means of Monte Carlo simulations. CT data volumes from 6 lung patients, with different lesion size, were processed and analyzed. The tumor region (generally the PTV) and low density voxels were segmented out to generate a new processed CT. A Digital Reconstructed Radiography (DRR) was computed from this processed CT volume. After equalizing the histogram between 0 and 1 of both particle radiography and DRR, the two images were subtracted thus obtaining a high signal around the tumor region. Contrast to Noise Ratio (CNR) was used as a metric to measure the enhancement. A normalized cross-correlation based algorithm was implemented to automatically detect the GTV area. The estimated center of mass (CM) of the GTV was compared to projection contours drawn by physicians. **Results:** CNR figures showed improvement up to 6 times when comparing the enhanced contrast image vs. the original particle radiography. The 2D distance between the real and the automatically estimated CM of the GTV was 2,12±0,62 mm (median±quartile). **Conclusions:** The advantage of using proton or carbon radiography to detect soft tissue during patient set up and radiation delivery can be further on improved by using prior knowledge derived from the planning CT. The method we propose is able to significantly enhance the contrast of the tumor region with acceptable computational time for real time applications. Further analysis is required to study the benefit of such a methodology to track the lesion over time during treatment. The authors declare that no conflicts of interest exist.

TH-E-BRA-06

Feasibility of Real Time MRI-Guidance in Proton Therapy

M Moteabbed*, J Schuemann, H Paganetti, Massachusetts General Hospital, Boston, MA

Purpose: To investigate the feasibility of in-vivo real-time MRI guidance as a potential treatment monitoring technique in proton therapy if such a system would be installed in a treatment room. **Methods:** The effect of MRI magnetic field on the proton dose distribution inside the patient anatomy was studied using the TOPAS (Tool for Particle Simulation) Monte Carlo (MC) tool. The right and left lateral fields for a prostate patient with 50 Gy prescribed dose (excluding the boost) were simulated based on the existing treatment plans using 0, 0.5 and 1.5 T uniform magnetic field in the superior-inferior direction. Dose Volume Histograms were compared for the CTV and several organs at risk (OARs) such as bladder, rectum and femoral heads. **Results:** Similar for both beams, lateral deflection of 2.5 and 7.3 cm was observed for 0.5 and 1.5 T fields at the end of range, respectively. It was found that an additional gantry rotation of 10 and 30 degrees could correct for the curved path of the proton beam. Therefore, the beams were re-simulated in the magnetic field, applying an anterior-posterior shift in the beam position. Using a beam position shift of 2.5 cm in the planning/delivery process could very well compensate for the magnetic field deflection in 0.5 T setting. The D95 varied by only 0.3 Gy. Also the OARs dose was maintained at the same level compared with the original treatment. However, the beams in 1.5 T field could not be well approximated by a simple shift of the field and the CTV and OAR doses were higher than prescribed. **Conclusions:** Since most existing open-MRI systems operate at or less than 0.5 T, proton-MRI treatments can be potentially planned by revising planned beam angles and considering MC-determined beam

and registered shifts. **Results:** For a 1mm discrepancy criterion between simulated and registered shifts, the success rates between OBI-DTS /Ref-DTS-FBCT, OBI-DTS /Ref-DTS-AIP, and OBI-DTS /Ref-DTS-4DCT registrations are 14.3%, 28.6%, and 100% for 2mm shifts, 0%, 14.3%, 100% for 5mm shifts, and 42.9%, 28.6%, 100% for 10mm shifts, respectively. **Conclusions:** The simulation study indicated that the phase-matched Ref-DTS-4DCT technique considerably improved the target verification accuracy than that provided by non-phase-information Ref-DTS-FBCT or Ref-DTS-AIP. Therefore, it has the potential to validate VMAT treatment of moving targets. (Research partially supported by grant from Varian Medical Systems) Research partially supported by grant from Varian Medical Systems.

TU-A-BRA-10

Real-Time Markerless Tumor Tracking with MV Imaging and a Dynamic Multi-Leaf Collimator (DMLC)

J Rottmann[1,2]*, P Keall[3], Y Yue[1], R Berbeco[1], (1) Brigham and Women's Hospital, Dana-Farber Cancer Institute and Harvard Medical School, Boston, MA, (2) German Cancer Research Center, Heidelberg, Germany, (3) University of Sydney, Sydney, Australia

Purpose: The implementation of a real-time adaptive therapy system. Automatic soft tissue localization (STiL) is used to drive DMLC adaptation maintaining the position of the dynamic treatment aperture relative to the tumor location during the entire breathing cycle. The STiL component utilizes electronic portal images and operates without the need for fiducial markers. The proposed system has the potential to improve treatment accuracy, dose conformity and sparing of healthy tissue. **Methods:** The system is implemented and tested on a clinical linear accelerator featuring an electronic portal imaging device (EPID) and a DMLC control system. EPID images are continuously acquired at a frame rate of 12.86 Hz. The STiL component processes the images in real-time, sending its output - the current tumor position - to the DMLC component, which moves the aperture to that position. Image transfer, tumor position calculation and DMLC motion introduce a time lag between tumor position at acquisition time and at the time the treatment aperture reaches this position. We analyze this latency with a dynamic chest phantom driving a 1D sinusoidal motion (20mm superior-inferior motion range and 4.5s period). We estimate the resulting average geometric systematic error in a clinical setting by driving the phantom with several patient traces (recorded from fiducial tracking during lung SBRT). **Results:** The individual geometric errors of the StiL and the DMLC component are each smaller than 1 mm. The overall system latency was found to be 210 ms. The average rms-error of 11 patients traces (172 beams) was found to be (1.8 ± 0.8) mm with this latency. **Conclusions:** We have implemented a real-time adaptive therapy system integrating automatic soft tissue tumor localization with DMLC adaptation of the treatment aperture. The functionality of the combined system was tested successfully and the systemic latency and resulting rms error measured. Varian Medical Systems Inc., NCI grant CA93626

TU-A-BRA-11

Targeted Drug Delivery Technique Employing Pulsed Focused Ultrasound for Treatment of Prostate

L Chen[1]*, N Rapoport[2], X Chen[1], D Cvetkovic[1], J Xue[3], q xu[4], X Tong[4], H Liu[5], R Gupta[2], C Ma[1], (1) Fox Chase Cancer Center, Philadelphia, PA, (2) University of Utah, Salt Lake City, UT, (3) Cancer Center of Union Hospital, Tongji Medical College of Huazhong Univers, Wuhan, (4) 3rd Affiliated Hospital of Qiqihar Medical University, Qiqihar, (5) Henan Provincial Cancer Hospital, Zhengzhou

Purpose: The purpose of this study is to investigate an innovative approach to prostate cancer therapy using nanodroplet-encapsulated drugs combined with pFUS (pulsed high intensity focused ultrasound) treatment. Pulsed FUS treatment provides a localized drug release from the carrier and enhanced intracellular uptake, which ensures temporal and spatial control of local drug delivery while lowering the systemic toxicity. **Methods:** LNCaP cells were implanted into the prostates of nude mice. Tumor growth was monitored using MRI. The tumor-bearing mice were randomly divided into 5 groups (n=3). Group 1, animals were treated with an IV injection of paclitaxel (PTX)-encapsulated nanodroplets (ND-PTX) + pFUS. Animals in Group 2 were treated with pFUS alone. Animals in Group 3 were injected (IV) with PTX-encapsulated nanodroplets alone, Group 4 received pFUS+empty nanodroplets and Group 5 was used as a control group. After treatment, animals were allowed to survive for 4 weeks. Tumor growth delay was monitored by MRI. The formulation of the PTX-encapsulated nanodroplets is as follows: PTX dose 20 mg/kg, Nanoemulsion composition 0.5% PTX, 1% perfluorocarbon and 2% stabilizing block copolymer. Ultrasound treatment parameters were 1MHz, 25W acoustic power, 10% duty cycle and 60 sec for each sonication. **Results:** Compared with the control group, significant tumor growth delay was observed in Group 1 with p=0.004, 3 weeks after treatment. There was no significant tumor growth delay observed for Group 2 (p=0.285), Group 3 (p=0.452) and Group 4 (p=0.158). **Conclusions:** Our preliminary results showed a great potential for prostate cancer therapy using targeted PTX+ nanodroplets, which could be activated by pFUS. More animal studies are warranted to confirm the results. The enhancement effect of pFUS on targeted drug delivery needs to be investigated quantitatively. This work is supported by Focused Ultrasound Surgery Foundation, DOD PC073127 and DOD BC102806. Technical support from InSightec is graciously acknowledged. funding supported partially by Focused Ultrasound Surgery Foundation, DOD PC073127 and DOD BC102806

Imaging Scientific Session — Room 213CD

Cone Beam CT 1

TU-A-213CD-01

GDRR: A GPU Tool for Cone-Beam CT Projection Simulations

X Jia*, H Yan, M Folkerts, S Jiang, University of California, San Deigo, La Jolla, CA

Purpose: Realistic calculations of x-ray projection images play an important role in many projects related to CBCT, such as the design of scanners and reconstruction algorithms. However, to yield a desired level of realism it usually requires a tremendously long computational time, which hinders the research process. The purpose of this project is to develop a realistic x-ray projection image simulation package, gDRR, on a computer graphics processing unit (GPU) to achieve both high accuracy and efficiency. **Methods:** Primary signals in a projection is computed by GPU-based ray-tracing algorithms, with many features considered, e.g. source energy spectrum, fluence map due to a bowtie filter, and detector response. Scatter signals are obtained by Monte Carlo (MC) simulations on GPU under the aforementioned realistic setup followed by a denoising step. Noise signals are calculated by taking the difference between the MC simulated primary and the ray-tracing primary signals, and the difference between the MC simulated scatter signals and the denoised scatter signals. The noise level is calibrated according to the mAs level in a scan. **Results:** The primary signals agree well with results from MC simulations. As for the scatter signals, our MC results for real patient cases are in good agreement with those from EGSnrc with less than 2% relative error using 10 million source photons. Various realistic artifacts can be observed in CBCT images reconstructed from the simulated projections, e.g. beam hardening, scatter, and noise. The computation time per projection is ~20ms for primary signal per energy channel, ~4sec for scatter signal, and 1~2sec for all other steps. **Conclusions:** We have developed a complete simulation package on GPU to compute x-ray projections in CBCT. Primary, scatter, and noise signals can be calculated with a high level of realism at a high efficiency. This work is supported in part by NIH (1R01CA154747-01), Varian Medical Systems through a Master Research Agreement, and the Thrasher Research Fund.

TU-A-213CD-02

Contrast-To-Noise Ratio (CNR) Enhancement and Lag Correction in Cone Beam CT (CBCT) Using a Synchronized-MOving-Grid (SMOG) System

L Ren[1]*, J Jin[2], F Yin[1], (1) Duke University Medical Center, Durham, NC, (2) Henry Ford Hospital System, Detroit, MI

Purpose: To develop a synchronized moving grid (SMOG) system to enhance the contrast-to-noise ratio (CNR) and correct image lag in cone-beam CT (CBCT). **Methods:** The SMOG system uses a rapidly oscillating, synchronized moving grid attached to the kV source. Multiple exposures are taken at each gantry angle with the grid offset by a distance equal to the grid interspace width after each exposure, before the gantry moves to the next position during a scan. In each projection image, patient image data are acquired within the grid interspace area and scatter is measured under the area blocked by the grid for post-scan scatter correction. The grid provides direct scatter reduction by blocking part of the beam, which enhances CNR in the reconstructed CBCT images. Image lag was also estimated from the

TU-C-BRB-03

Monte Carlo Study of a Compact Distributed X-Ray Source Microbeam Radiation Therapy Research Irradiator

E Schreiber*, S Chang, UNC School of Medicine, Chapel Hill, NC

Purpose: Microbeam radiation therapy (MRT) is a promising experimental treatment modality produced by large synchrotron facilities. Using carbon-nanotube (CNT) field emission based x-ray generation as an enabling technology, we propose a compact MRT small animal irradiator. We report on a Monte Carlo feasibility study of the proposed device. **Methods:** A prototype 160 kVp CNT MRT device was simulated using EGSnrc-based codes. Dosimetry for 100-micron thick planar beams at 160 mm SSD was calculated in a 30 mm diameter cylindrical water target. In contrast to single source synchrotron MRT systems, the proposed CNT-MRT system has multiple linear x-ray sources were arranged in a ring surrounding the target. The planar dosimetry from the MRT was simulated by using 12-24 equally spaced identical linear x-ray source segments. Dosimetry for the full MRT array was generated by combining circular planar dose distributions in parallel planes separated by 150-1000 microns. The resulting configurations were analyzed for isocentric dose rate, dose to normal tissue, and peak-to-valley ratio. **Results:** The peak-to-valley dose ratio varied from 10 to 100 as the spacing between adjacent parallel microbeams was increased from 150 to 1000 microns. The dose rate at the center of the phantom was calculated to be 700 Gy/A/min per linear source segment. An expected maximum current per source segment of 1 A (due to anode heating) projects a maximum dose rate of 280 Gy/sec at isocenter for a 24-source segment configuration. The dose rate falls by 80% within 5 mm of the edge of the target area in the center of the phantom, providing significant normal tissue sparing compared with single-direction MRT techniques. **Conclusions:** Monte Carlo simulations show that it is feasible for the proposed MRT device to produce the dose rate and peak-to-valley characteristics needed to conduct MRT research. This work is supported by NCI grant 1U54CA151652

TU-C-BRB-04

A Monte Carlo-Based Small Animal Dosimetry Platform for Pre-Clinical Trials: Proof of Concept

B Bednarz*, A Besemer, Y Yang, University of Wisconsin, Madison, WI

Purpose: The development of novel agents for targeted radionuclide therapy has led to an important need for accurate dosimetry characterization during pre-clinical trials. The purpose of this study is to discuss our progress in developing a fully automated Monte Carlo-based dosimetry platform for external and/or internal absorbed dose quantification in small animals. **Methods:** The dosimetry platform was built entirely around the Monte Carlo code Geant4 version 9.3. CT and PET image datasets of a mouse injected with CLR1404, a novel tumor target pharmaceutical that is tagged with both I-124 and I-131 for imaging and therapy, were used for this preliminary study. The activity distribution in the tumor acquired from the PET scan was modeled as a simple spherical source. The same CT image set was used to generate external dose distributions from a 6 MV photon beam spectrum. **Results:** The external dose distributions from the 6 MV photon source and the internal dose distributions from CLR1404 were combined to get a relative dose distribution within the mouse. **Conclusions:** We provided a proof-of-concept for a fully automated dose calculation platform in small animals that can be used for developing protocols for pre-clinical trials. We are currently working on additional modifications to better represent both the external beam source for our small animal irradiator as well as the activity distributions gathered by the PET scan.

TU-C-BRB-05

BEST IN PHYSICS (THERAPY) - Combined Effects of Pulsed Non-Thermal Focused Ultrasound and Radiotherapy for Prostate Cancer Treatment

X Chen[1], D Cvetkovic[1], J Xue[1,2], L Chen[1], C-M Ma[1], (1)Radiation Oncology Department, Fox Chase Cancer Center, Philadelphia, PA, (2)Cancer Center of Union Hospital, Tongji Medical College of Huazhong University of Science and Technology, Wuhan, China

Purpose: Recent studies have shown non-thermal effects of pulsed focused ultrasound (pFUS) on tumor growth control. This study is to investigate the combined effects of non-thermal pFUS and radiotherapy (RT) for prostate cancer treatment. **Methods:** Animal prostate tumor model was developed by implanting LNCaP cells in mice prostates. Tumor-bearing mice were randomly assigned to 3 groups (n=8): (1) pFUS; (2) pFUS+RT; (3) control. MR-guided pFUS treatment was performed using InSightec ExAblate 2000 system with a 1.5T GE MR scanner. Non-thermal sonications were delivered by keeping the body temperature <42°C as measured real-time by MR thermometry. Prostate tumors in groups 1 and 2 were exposed to pFUS (1MHz, 25W focused ultrasound; 1Hz pulse rate with a 10% duty cycle) for 60 sec for each sonication. Each tumor was covered entirely using 4-8 sonication spots. Prostate tumors in group 2 also received 2 Gy radiation dose within 30 minutes after pFUS treatment using Siemens Artiste (6MV photon energy, 300MU/min dose rate). Following the treatment, mice were scanned weekly using MRI for tumor volume measurement. **Results:** Tumor volumes in the control group showed exponential increase from 121±5 mm^3 on treatment day to 172±9, 247±15, 344±28, and 500±42 mm^3 at 1, 2, 3, and 4 weeks post treatment, respectively. In contrast, tumor volumes in the pFUS group were 33% ($p<0.05$), 29% ($p<0.05$), 14%, and 15% smaller, and the pFUS+RT group were 31%, 31%, 26%, 33% smaller ($p<0.05$) at week 1, 2, 3, and 4 post treatment, respectively. Both pFUS and pFUS+RT groups showed significant tumor growth delay in the first two weeks. **Conclusions:** Our study showed that pFUS combined with radiotherapy can significantly delay the tumor growth. Radiation after pFUS treatment provided an additional benefit for tumor control (sponsored by Focused Ultrasound Surgery Foundation, Varian Medical Systems, DOD PC073127, DOD BC102806).

TU-C-BRB-06

A Multipurpose Quality Assurance Phantom for the Small Animal Radiation Research Platform (SARRP)

W Ngwa*, P Tsiamas, P Zygmanski, M Makrigiorgos, R Berbeco, Brigham and Women's Hospital, Dana Farber Cancer Institute, Harvard Medical School, Boston, MA

Purpose: The suitability and performance of a mouse-size MOSFET ('Mousefet') phantom is investigated for routine quality assurance (QA) of the Small Animal Radiation Research Platform (SARRP). **Methods:** The Mousefet phantom was constructed by custom integration of 5 micro MOSFETS, arranged in a quincunx pattern, within a miniature tissue equivalent phantom. The phantom was designed to facilitate SARRP QA tasks which may warrant daily evaluation: output constancy, isocenter congruency test, and cone beam computed tomography (CBCT) image geometric accuracy. For output constancy the phantom was irradiated with an open field and all 5 micro-MOSFET readings taken. For the isocenter congruency test, an appropriate size collimator was used to irradiate one of the MOSFETs, imaged and positioned at CBCT isocenter. The acquired CBCT image was then used to verify image geometric accuracy and other image quality parameters. Sample data from 10 days in a period of over one month was compared to reference measurements and evaluated for daily variation. **Results:** Output constancy measurements showed maximum daily variation of less than 3% for all MOSFETS, in consonance with observations from concurrent ion chamber measurements. The design of the Mousefet phantom allows the output check data to be used for prompt verification of beam energy and cone profile constancy. For the isocenter congruency test, it is demonstrated that the Mousefet Phantom can detect 0.3 mm deviations of the CBCT isocenter from the radiation isocenter. Meanwhile, results for CBCT image geometric accuracy were consistently found to be within 2% of the expected value. Other CBCT image-quality parameters could also be assessed in terms of image intensity constancy, noise and image uniformity. **Conclusions:** Overall, the results establish the Mousefet phantom as a simple and time-efficient multipurpose tool that could be employed effectively for routine quality assurance of the SARRP.

TU-C-BRB-07

Comparison of Preclinical and Clinical Conformal Radiation Therapy Techniques and Protocols to Establish a Translational Pathway

S G Price[1,2]*, D Rangaraj[1,2], S Yaddanapudi[2], E W Izaguirre[1,2], (1) Nuclear Science and Engineering Institute, University of Missouri, Columbia, MO (2) Washington University School of Medicine, Saint Louis, MO

Purpose: The purpose of this study was to compare the techniques and protocols used in clinical radiation therapy and recently developed preclinical image guided micro irradiation to establish a link between small animal conformal irradiation and clinical treatment protocols. This work will establish protocols that, according to treatment site, will facilitate the translation of conclusions from radiobiological experiments to clinical

calibration, implementation of aMC into a treatment planning systems and applications for IMPT optimization.

Learning Objectives:
1. Understanding the physics principles underlying current semi-empirical proton dose computation models, their assumptions and approximations and their effect on accuracy.
2. Appreciating the potential impact of approximations on clinical outcomes.
3. Understanding the role of Monte Carlo techniques in identifying the causes of differences between results of semi-empirical models, measurements and Monte Carlo and in the development of more accurate algorithms.
4. Learning about the current status of Monte Carlo and abridged-Monte Carlo techniques for clinical use.

Conflicts of interest: Mohan – Research grant from Philips. Soukup – Elekta employee.

Imaging Symposium Room 217BCD
Advanced Imaging Applications and Contrast Agents in Ultrasound Imaging

TH-C-217BCD-01
BEST IN PHYSICS (IMAGING) - Evaluation of Apoptosis and Proliferation in Non-Thermal Pulsed HIFU Treated Mouse Prostate Tumors

D Cvetkovic*, X Chen, C Ma, L Chen, Fox Chase Cancer Center, Philadelphia, PA

Purpose: The underlying mechanism of non-thermal effects of pulsed high intensity focused ultrasound (pFUS) on normal and tumor tissues is not well understood. Our recent studies showed significant prostate cancer cell killing in vitro and significant prostate tumor growth delay in vivo after pFUS treatment. We hypothesized that these effects of non-thermal pFUS are due to an increase in cell apoptosis and decrease in cell proliferation. Therefore, the purpose of this study was to analyze the biomarkers of apoptosis and proliferation in prostate tumors after pFUS exposures. **Methods:** An orthotopic prostate tumor model was established in nude mice. Prostate tumors were sonicated with MR guided pFUS (1MHz, 5W acoustic power, 5Hz frequency; 0.1duty cycle) for 60 sec for each sonication with temperature <42°C (InSightec ExAblate 2000 with a 1.5T GE MR scanner). Untreated tumors were used as controls. The mice were sacrificed at predetermined times up to 7 days following therapy. Tumors were processed for light microscopic examination with H&E staining and immunohistochemical staining for caspase 3 (a marker of apoptosis) and Ki67 (aproliferation marker) expression. **Results:** Light microscopy revealed the absence of thermal damage and acute destruction of tumor tissues exposed to pFUS. The microvessel walls in the tissues remained intact. There was no change in the extent of hemorrhage upon pFUS treatment over time. The apoptotic index, defined as a percentage of apoptotic cells per total number of cells, peaked at 24 hours after FUS treatment relative to control. There was no dramatic difference in the proliferation indices between different time points. **Conclusions:** Our results suggested that non-thermal pulsed pFUS induced caspase 3-mediated apoptosis and did not produce any thermal damage in the prostate tumor tissues. We are performing additional studies to evaluate blood vessel density and cellular DNA damage upon pFUS treatment.

TH-C-217BCD-02
Ultrasound Texture Analysis of Radiation-Induced Parotid-Gland Injury in Post-Radiotherapy Head-And-Neck Patients: Feasibility Study

X Yang*, S Tridandapani, J Beitler, D Yu, S Henry, H Chen, W Curran, T Liu, Emory University, Atlanta, GA

Purpose: Xerostomia (dry mouth), resulting from radiation damage to the parotid glands, is one of the most common and distressing side effects of head-and-neck cancer radiotherapy. We have developed a family of sonographic texture features to evaluate the morphologic and microstructural integrity of the parotid glands, and investigate the feasibility of quantitative evaluation of radiotherapy-induced parotid-gland injury. **Methods:** In this pilot study, 12 post-radiotherapy head-and-neck cancer patients and 7 healthy volunteers were enrolled. Each participant underwent one ultrasound study, and longitudinal (vertical) ultrasound scans were performed of the bilateral parotids. The averaged follow-up time for the post-radiotherapy patients was 17.2 months and the median radiation dose was 32.3 Gy. Eight grey level co-occurrence matrix (GLCM) features were derived from the B-mode images. The associated parameters for texture features can be summarized as follows: 1. Inverse differential moment (IDM): local homogeneity; 2. Contrast: difference of gray-scale through continuous pixels of the image; 3. Angular second moment (ASM): homogenous texture; 4. Entropy: disorder of the image. 5. Variance: heterogeneity; 6. Correlation: linear relationship between the gray-scale of pixel pairs; 7. Cluster shade and 8. Cluster prominence: the perceptual concepts of uniformity and proximity. **Results:** Significant differences ($p<0.05$) were observed in 8 sonographic features, between normal and irradiated parotid glands. IDM value decreased from 7.88±1.14E-2 (normal) to 6.93±1.54E-2 (irradiated); Contrast value increased from 3.41±1.11E+2 to 8.45±3.46E+2; ASM value decreased from 6.06±1.72E-4 to 3.02±0.87E-4; Entropy value increased from 7.66±0.34 to 8.47±0.23; Variance value increased from 2.84±1.01E+2 to 9.30±3.53E+2; Correlation value decreased from 1.35±0.45E-3 to 6.22±2.09E-4; Cluster shade value increased from 1.20±1.24E+4 to 1.51±1.27E+5; Cluster prominence value increased from 3.11±2.50E+6 to 3.74±3.11E+7. **Conclusions:** This work has demonstrated the feasibility of ultrasonic texture evaluations of the parotid glands, and the sonographic features may serve as imaging signatures to assess radiation-induced parotid damage.

TH-C-217BCD-03
Evaluation of the Spatial Resolution and Noise Properties of a Prototype Transmission Ultrasound Imaging System Employing An Acousto-Optic (AO) Detector

J.R. Rosenfield*[1], J.S. Sandhu[2], J.K. Tawiah[2], and P.J. La Riviere[1], (1) The University of Chicago, Chicago, Illinois, (2) Santec Systems Inc., Arlington Heights, IL

Purpose: In this work, the spatial resolution and noise properties of a prototype full-field transmission ultrasound imaging system employing an acousto-optic (AO) liquid crystal detector were characterized. The AO effect is a phenomenon in which an incident acoustic wave field induces local birefringence changes in a liquid crystal. These birefringence changes manifest as brightness changes when the liquid crystal is optically illuminated using polarized light, thus providing spatial information about the field. **Methods:** A compressed, Zerdine-based breast phantom containing 12 artificial spherical lesions was imaged using plane-wave ultrasound illumination. Lesions of diameter 2 mm, 4 mm, 6 mm, and 8 mm were embedded at depths of 12.7 mm, 25.4 mm, and 38.1 mm within the phantom background. To minimize coherence artifacts, the transducer frequency was swept continuously from 3.25 MHz to 3.45 MHz at a rate of 100 MHz/s. The transducer voltage was ramped from 0.1 V to 6.5 V to permit identification of the onset of the AO effect in the detector. An analysis of image quality was performed on 50 identically acquired images in which the contrast-to-noise ratio was determined for each lesion in the mean acquired image. Apparent lesion size was also computed as a function of distance from the AO detector. **Results:** The spatial resolution analysis revealed that lesion size in the mean acquired image increased linearly with lesion-to-detector distance. Extrapolation of the least squares regression lines for apparent lesion size versus lesion-to-detector distance to zero distance agreed well with the actual lesion sizes. The noise analysis demonstrated that a contrast-to-noise ratio of 13.1 could be obtained with the prototype system for the transducer settings and phantom properties considered. **Conclusions:** This investigation indicates the potential for incorporating a liquid crystal AO detector into a transmission ultrasound system for full-field breast imaging.